Identification and characterization of

the *RIB1* gene involved in nitric oxide tolerance

in *Saccharomyces cerevisiae*

Khairul Anam

Nara Institute of Science and Technology (NAIST)
Graduate School of Biological Sciences
Laboratory of Applied Stress Microbiology
Prof. Hiroshi Takagi

Graduate School of Biological Sciences　　　　　　　Doctoral Thesis Abstract

Laboratory (Supervisor)	Applied Stress Microbiology (Prof. Hiroshi Takagi)		
Name (surname) (given name)	Anam Khairul	Date	2019/07/29
Title	Identification and characterization of the *RIB1* gene involved in nitric oxide tolerance in *Saccharomyces cerevisiae* (酵母の一酸化窒素耐性に関与する *RIB1* 遺伝子の同定と特性解析)		

Nitric oxide (NO) is a small signaling molecule that plays roles in a number of biological processes. In mammalian cells, NO is generally produced by NO synthase (NOS) from L-arginine. The physiological functions of NO mainly occur through activation of soluble guanylyl cyclase and the post-translational modification of the proteins in mammalian cells. Meanwhile, the molecular actions of NO depend on having a microenvironment in which NO can function. NO can react with not only with various molecules, including metal ions, heme group, thiols, or other free radicals, but also with proteins through *S*-nitrosylation at the cysteine residues.

In the yeast *Saccharomyces cerevisiae*, a microorganism that is important as a model for higher eukaryotes and in the fermentation industry, NO was shown to generate in the cell despite the absence of NOS orthologous genes in the genome. A previous study in our laboratory suggested that NO production from L-arginine induced by temperature up-shift requires NOS-like activity of the flavoprotein Tah18 in *S. cerevisiae*. Gene knockdown analysis also indicated that Tah18-dependent NO synthesis confers high-temperature stress tolerance on yeast cells. However, NO produces cytotoxicity at a higher level by generation of NO-derivatives, especially reactive nitrogen species (RNS) such as peroxynitrite ($ONOO^-$) from its reaction with superoxide anion. This leads to nitrosative stress, in which an excessive level of RNS including NO cannot be neutralized. RNS interrupt the activities of various proteins, promoting cell damage and death. Therefore, the complexities of NO actions and NO responses demand attention in order to overcome excessive NO for cell protection.

Several mechanisms are involved in NO tolerance in yeast. First, there is the stress response of enzymes involved in the glutathione and thioredoxin systems (both of which show functions similar to those in the mammalian systems) through transnitrosylation and denitrosylation processes. Second, an NO oxidoreductase flavohemoglobins (Fhb) converts NO into nitrate or nitrous oxide by oxidation or reduction, respectively. However, the molecular mechanisms of NO tolerance in yeast are not yet fully understood. Therefore, the research objective of this study is to find the novel gene(s) required for NO tolerance, and to clarify its molecular mechanisms in yeast.

For this study, I use the multicopy plasmid library harboring the digested genomic DNA of *S. cerevisiae* X2810-1A strain and the acidified NO_2^- condition ($NaNO_2$ at pH 5.5) to screen for the novel genes required for NO tolerance. Preliminary experiments showed that the acidified NO_2^- condition generated NO and induced growth defects in yeast cells in a concentration-dependent manner, suggesting that excessive NO is produced by such conditions. More than 160,000 colonies of transformants in the plasmid library were screened, and approximately 400 colonies that showed better growth than the cells harboring the empty vector under acidified NO_2^- conditions were selected as candidates with NO tolerance. Finally, plasmids were extracted from the 4 candidates that all harbored the common DNA fragments containing the *RIB1* gene.

The *RIB1* gene encodes a GTP cyclohydrolase II (GTPCH2/Rib1p) responsible for the first

step of riboflavin (RF) biosynthesis. Then, to confirm that *RIB1* is important for the NO tolerance of yeast cells, I analyzed the phenotype of the *RIB1* overexpressing (RIB1-OE) cells. RIB1-OE cells grew faster than wild-type (WT) cells under the acidified NO_2^- condition. On the other hand, to examine the phenotype of the *RIB1*-deleted (Δ*rib1*) cells, Δ*rib1* cells were cultured in a medium supplemented with RF because they can survive in its presence, which is essential for cell growth. I found that Δ*rib1* cells showed higher sensitivity to acidified NO_2^- than WT cells. Furthermore, the addition of RF did not affect the phenotypes of any of the cells tested, including WT, RIB-OE, or Δ*rib1* cells. These results imply that the *RIB1* gene confers NO tolerance on yeast cells, regardless of RF synthesis.

To investigate the crosslink between Rib1p and denitrosylation enzymes in thioredoxin and glutaredoxin systems, I evaluated the effect of the *RIB1* overexpression on single gene-deleted cells, including Δ*grx1*, Δ*grx2*, Δ*glr1*, Δ*trx1*, Δ*trx2*, Δ*trx3*, and Δ*trr2*, under the acidified NO_2^- condition. Overexpression of *RIB1* enhanced tolerance to acidified NO_2^- in all of the gene-deleted cells to the same degree as WT cells, suggesting that there are no genetic interactions between Rib1p and thioredoxin/glutaredoxin systems for NO tolerance.

I next focused on the importance of Rib1p enzymatic activity for NO tolerance. In the Rib1p molecule, three cysteine residues at positions 148, 159, and 161 play an important role in the enzymatic activity of Rib1p. The overexpression of Rib1p-variants (Cys148Ser, Cys159Ser, and Cys161Ser) did not enhance tolerance to acidified NO_2^-, even though Western blot analysis showed that the intracellular protein level of each variant was almost the same. This suggested that the important factor for protecting yeast cells from excessive NO is not the Rib1 protein itself but its enzymatic activity. Furthermore, intracellular NO level was measured after treatment with an NO donor NOC-5. Yeast cells treated with the cell-permeable NO-specific fluorescence probe DAF-FM DA were incubated with NOC-5, followed by estimation of intracellular fluorescence intensity by flow cytometry. The NO level in RIB1-OE cells was lower than that in WT cells, suggesting that *RIB1* overexpression decreased the NO level in yeast cells.

Subsequently, to examine the possibility that Rib1p quenches NO directly or indirectly, a recombinant Rib1p (rRib1p) was expressed and purified using the plasmid pET53 and *Escherichia coli* Rosetta (DE3) strain. The DAF-FM probe was incubated with NOC-5 and fluorescence was monitored with a fluorescence spectrophotometer to analyze the NO quenching ability of the samples. Fluorescence increased in a time-dependent manner, regardless of the presence of Rib1p, suggesting that Rib1p does not have the ability to directly scavenge NO. In general, Rib1p converts GTP to 2,5-diamino-6-(1-D-ribosylamino)pyrimidin-4(3H)-one 5'-phosphate (DARP), formate, and pyrophosphate. Therefore, I investigate whether the reaction products of Rib1p, including DARP, could scavenge NO. The WT rRib1p was incubated with GTP, followed by boiling to denature rRib1p, to prepare the rRib1p reaction products. Interestingly, the addition of the rRib1p reaction products dramatically decreased the time-dependent increase of fluorescence induced by NOC-5. On the other hand, the addition of formate or pyrophosphate did not affect the rate of increase of fluorescence. Furthermore, the reaction mixture prepared using the variant rRib1p (Cys148Ser) did not decrease fluorescence. These results indicate that DARP directly quenches NO. Altogether, I propose a model of the Rib1p-dependent NO tolerance mechanism in which DARP synthesized by Rib1p from GTP reacts with NO to scavenge it, confering the NO tolerance in *S. cerevisiae*.

TABLE OF CONTENTS

LIST OF FIGURES

LIST OF TABLES

LIST OF ABBREVIATIONS

NO	:	Nitric oxide
ARIP	:	5-Amino-6-(ribitylamino)uracil (Rib2p product)
DAF-FM	:	4-Amino-5-methylamino-2',7'-difluorofluorescein
DAF-FM DA	:	4-Amino-5-methylamino-2',7'-difluorofluorescein diacetate
DAF-FM-T	:	DAF-FM triazole
DARIP	:	2,5-Diamino-6-(5-phospo-D-ribitylamino)-pyrimidin-4(3H)-one (Rib7p product)
DARP	:	2,5-Diamino-6-(5-phospo-D-ribosylamino)-pyrimidin-4(3H)-one (Rib1p product)
DARPM	:	DARP moiety analog: 2,4,5-triamino-6-hydroxy-pyrimidine
DETA-NONOate	:	Diethylenetriamine NONOate (an NO donor)
DHBP	:	3,4-Dihydroxy-2-butanone-4-phosphate (Rib3p product)
EDRF	:	Endothelial derived relaxing factor
EV	:	Empty vector
FAD	:	Flavin adenine dinucleotide
FHb	:	Flavohemoglobin
FMN	:	Flavin mononucleotide
GC	:	Guanylate cyclase
Glr	:	Glutathione reductase
Grx	:	Glutaredoxin
GSH	:	Glutathione
GSNO	:	*S*-Nitrosoglutathione
GSNOR	:	*S*-Nitrosoglutathione reductase
GSSG	:	Glutathione disulfide
GTP	:	Guanosine triphosphate
GTPCH2	:	Guanosine triphosphate cyclohydrolase II
NADP	:	Nicotinamide adenine dinucleotide phosphate
NADPH	:	Reduced form of NADP
NOC-5	:	3-[2-Hydroxy-1-(1-methylethyl)-2-nitrosohydrazinyl]-1-propanamine (an NO donor)
NOD	:	Nitric oxide deoxygenase

NOS	:	Nitric oxide synthase
OD	:	Optical density
PKG	:	Protein kinase G
PVDF	:	Polyvinylidene difluoride
RF	:	Riboflavin
RIB1-OE	:	*RIB1* overexpression
RIB1-RIB7-OE	:	*RIB1* and *RIB7* co-overexpression
RNS	:	Reactive nitrogen species
ROS	:	Reactive oxygen species
Rib1p	:	Rib1 protein/GTP cyclohydrolase II in *S. cerevisiae*
SD	:	Synthetic defined (medium)
s.d	:	Standard deviation
SDS-PAGE	:	SDS-polyacrylamide gel electrophoresis
SNO	:	*S*-Nitrosothiols
Trr	:	Thioredoxin reductase
Trx	:	Thioredoxin
cGMP	:	Cyclic guanosine monophosphate
e-NOS	:	Endothelial NOS
i-NOS	:	Inducible NOS
n-NOS	:	Neuronal NOS
sGC	:	Soluble GC
WT	:	Wild-type

1. INTRODUCTION

1.1. Physiological functions of nitric oxide

Nitric oxide (NO) is a small signaling molecule involved in various biological processes. As a free radical gaseous molecule, NO is highly reactive and capable of reacting with a variety of molecules, both extracellularly and intracellularly. The first biological role of NO was revealed to be that of a vasodilator of blood vessels, after NO was identified as an endothelial derived relaxing factor (EDRF). Nitroglycerin, a medicine to treat angina patients, is thought to release NO, which mediates its pharmacological effect (Thippeswamy et al. 2006; Lima et al. 2010). Since then, various studies have been performed to analyze the diverse effects of NO
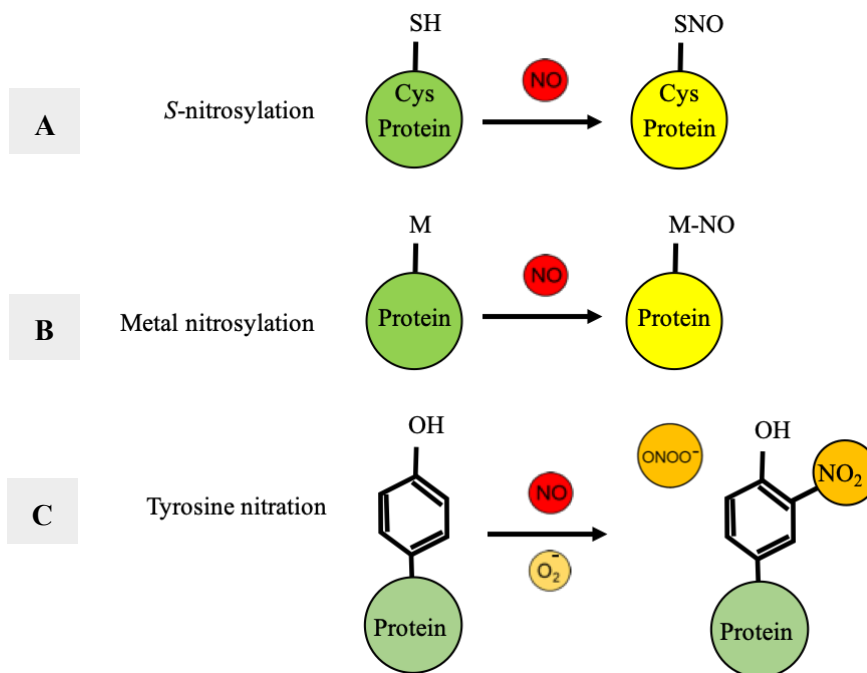
Figure 1. Types of post-translational modification by NO.
A. *S*-Nitrosylation of protein by NO at the thiol-group of the cysteine residue, **B.** Metal nitrosylation, **C.** Combination with superoxide, which forms peroxynitrite and nitrates the tyrosine residue.

Recently, various studies have highlighted the function of NO as a signaling molecule, which mediates intracellular effects. The molecular actions of NO depend on the microenvironments in which it functions (Cooper 1999; Feng et al. 2013; Hromatka

et al. 2005; Lu et al. 2014). In cells, NO can react with other radical molecules and generate more reactive secondary products, which also include RNS. RNS are capable of reacting with proteins, which possess free sulfhydryl groups at cysteine residues, reacting with tyrosine residues or with metals and heme to perform nitrosylation and nitration processes (Ridnour et al. 2004) (Figure 1). Nitrosylation influences protein activities and protein-protein interaction, as well as protein localization (Benhar et al. 2009). Despite various studies that have been conducted on NO, many aspects related to the mechanisms involved in overcoming the negative effect of cellular NO have not yet been established.

1.2. Synthesis and degradation/detoxification of NO

In mammalian cells, NO is endogenously synthesized from L-arginine by the enzymatic reaction of NO synthase (NOS). L-Arginine is oxidized to form L-citrulline and NO, and NADPH and oxygen are involved in the reaction. There are 3 different NOS isoforms produced by the different cell types that catalyze the reaction: endothelial NOS (e-NOS), neuronal NOS (n-NOS), and inducible NOS (i-NOS). These different NOS isoforms mediate NO biosynthesis for different purposes (Brown 2001; Förstermann and Sessa 2012).

NO production by e-NOS, as described previously, is important for the relaxation of blood vessels, which is important in patients with cardiovascular diseases. In addition, vasodilation of blood vessels is crucial in the male reproductive system. The NO effect takes place via the paracrine mechanism, in which NO is produced by endothelial cells and then diffuses into the smooth muscle cells. NO reacts with membranous guanylate cyclase (GC) to increase the production of cyclic guanosine monophosphate (cGMP), which consequently activates protein kinase G (PKG) and promotes relaxation of muscle cells. On the other hand, NO production by n-NOS takes part in the neurotransmitter released by neuronal cells via an autocrine mechanism and interaction with soluble GC (sGC) to promote cGMP production and induce cGMP-dependent signaling (Denninger and Marletta 1999; Thippeswamy et al. 2006). Meanwhile, NO production by i-NOS in the activated macrophages is a part of a non-specific immune response to eradicate pathogens including bacteria, yeast, and fungi. However, a high level of NO exhibits cytotoxic effects. Excessive NO production by any NOS isoforms can harm the body,

generating destructive conditions such as autoimmune or degenerative diseases (Gu et al. 2010).

NO activities are also involved in post-translational modification through *S*-nitrosylation of intracellular proteins (Hess et al. 2005; Hess and Stamler 2012). NO, produced by cells or from exogenous NO, reacts with protein thiols to form protein *S*-nitrosothiols (SNO), or with glutathione (GSH) to form *S*-nitrosoglutathione (GSNO); the later plays a role in the NO pool as GSNO transnitrosylates the other protein to form other SNO. Through this mechanism, several nitrosylated proteins modulate their downstream for upregulation or downregulation, and induce cGMP independent signaling. The nitrosylation processes are effective for cells if they can keep these processes under homeostasis conditions.

To maintain homeostasis, the denitrosylation process is established (Sengupta and Holmgren 2012; Benhar et al. 2009; Zaffagnini et al. 2013). Nitrosylation is a reversible process where the target protein with *S*-nitrosylation can be transformed back to its reduced form (Figure 2). These transnitrosylation and denitrosylation processes consist of many enzymes in the GSH and thioredoxin (Trx) systems. Both GSH and Trx reduce the *S*-nitrosylated protein back to its reduced form. The role of *S*-nitrosoglutathione reductase (GSNOR), which converts GSNO into glutathione disulfide (GSSG) by a reaction with GSH and NADH, is important in maintaining homeostasis. GSSG is then converted into GSH by glutathione reductase (Glr) with NADPH. In this mechanism, GSNOR also plays a role in converting NO, which nitrosylates GSH as GSNO, into nitrate. Meanwhile, through transnitrosylation, Trx reacts with the protein SNO to its oxidized form and releases free NO. The oxidized form of Trx is converted back into its reduced form by Trx reductase (Trr) in the presence of NADPH. However, when a high level of RNS (or ROS) is present and GSH and Trx are involved and cannot neutralize those compounds, nitrosative stress can occur and cause cells damage or death.
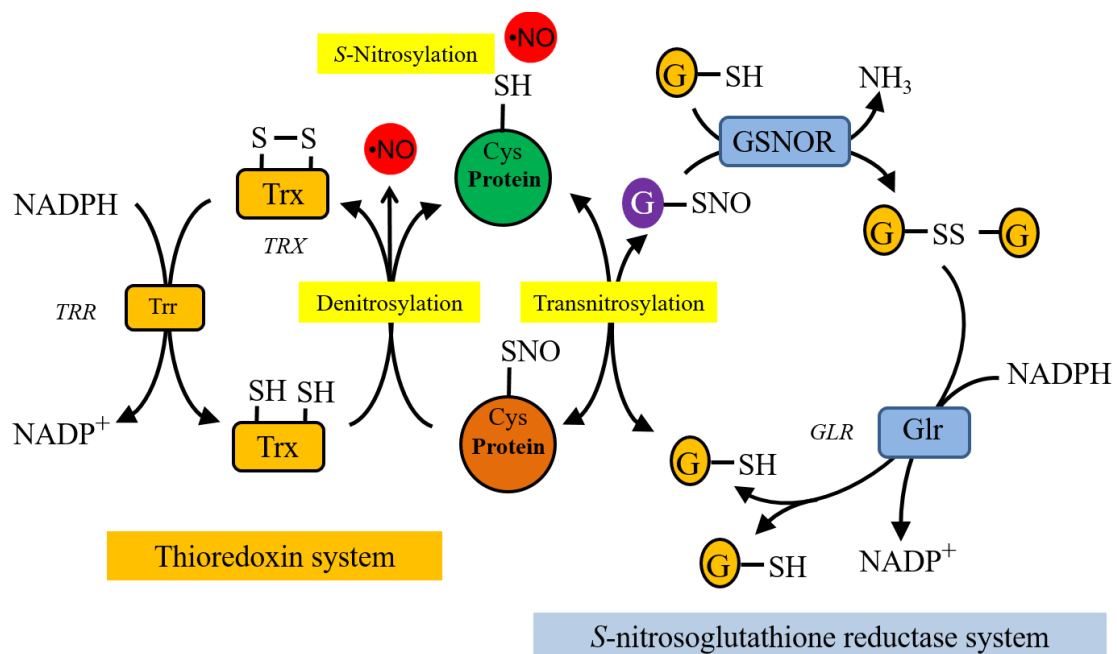
Figure 2. *S*-nitrosylation and denitrosylation processes involving thioredoxin and glutathione system. (Adapted from Benhar et al. 2009)

These acronyms were stand for, Trx = thioredoxin; Trr = thioredoxin reductae; GSNOR = *S*-nitrosoglutathione reductae; GSSG = glutathione disulfide; Glr = glutathione reductase; SH stands for reduced form of cysteine residue, meanwhile, SS was oxidized form of the cysteine residue. SNO indicates of nitrosylated cysteine residue. NADPH is reduced form of NADP, which stands for nicotinamide adenine dinucleotide phosphate.

NO plays dual functions in unicellular organisms and plants in a concentration-dependent manner. In bacteria, a low nanomolar cellular level of NO contributes to the self-defense against oxidative stress (Gardner et al. 1998; Gardner et al. 2000). At this level, NO also regulates the formation of biofilm in bacteria, including *Bacillus* sp. and *Staphyllococcus* sp., thus promoting bacterial colony formation. NO is also involved in toxin synthesis in *Streptomyces* strains (Allain et al. 2011). In contrast, at a higher level, NO could be toxic and induce cell death (Poole 2005). In yeasts, a low level of NO mediates resistance to oxidative and temperature stress (Nishimura et al. 2013; Nasuno et al. 2014; Liu et al. 2015). On the other hand, at a high micromolar level, NO could promote more severe oxidative and nitrosative stress (Tillmann et al. 2011; Almeida 2007). In plants, a low level of NO is also important for resistance to oxidative stress (Considine et al. 2015).

Table 1. Summary of dual NO functions in bacteria, yeast, human and plant

Organism	Low NO level	High NO level
Bacteria	➢ Resist oxidative stress. ➢ Regulate biofilm formation. ➢ Toxin synthesis. (Allain et al. 2000)	➢ Nitrosative stress and cell death. (Poole 2005)
Yeast	➢ Resist oxidative stress ➢ Resist high-temperature stress (Nishimura et al. 2013; Nasuno et al. 2014; Liu et al. 2015)	➢ Nitrosative stress and cell death. (Tillmann et al. 2011; Almeida 2007)
Human	➢ Resist oxidative stress. ➢ Vasodilation of smooth muscle cells. ➢ Neurotransmitter release. (Benhar et al. 2009)	➢ Nitrosative stress and cell death. ➢ Autoimmune and degenerative diseases (Gu et al. 2010)

1.3. Excessive NO induces nitrosative stress condition

As described previously, NO possesses biphasic effects depends on its intracellular level (Benhar 2015). Despite its protective roles at a lower level, NO is toxic when it exceeds levels with which cells can cope. At high levels, NO generates other RNS such as peroxynitrite from its reaction with superoxide anions (Ferrer-sueta and Radi 2009). Furthermore, abundant NO and other RNS lead to a nitrosative stress condition, under which cells cannot neutralize and eliminate the excessive NO and RNS. These molecules interrupt activities of various proteins through *S*-nitrosylation or tyrosine (Tyr) nitration, which induces loss of ATP production and cell death or apoptosis (Thippeswamy et al. 2006).

The budding yeast *Saccharomyces cerevisiae*, an industrial fermentation yeast, is an important microorganism that has been widely used as a model for higher eukaryotes. *S. cerevisiae* cells have a short life cycle and can survive under various experimental conditions. Its genomic information and sequences are also available. In terms of excessive NO responses, several kinds of yeasts, such as *Candida albicans*, are able to hinder apoptosis (programmed cell death), whereas the benign yeast, *S. cerevisiae* and *Schizosaccharomyces pombe* are more sensitive to excessive NO (Majumdar et al. 2012; Tillmann et al. 2011). Therefore, by using *C. albicans*, it is possible to find endogenous

mechanisms to resist excessive NO, whereas utilization of *S. cerevisiae* or *S. pombe* allows the external interventions or treatments with the aim of discovering novel mechanisms for excessive NO tolerance.

Unlike mammalian cells, yeast cells do not possess NOS. However, it has been reported that Tah18 of *S. cerevisiae* shows NOS-like activity (Nishimura et al. 2013; Yoshikawa et al. 2016). NO production mediated by Tah18 is within a low level of NO, which is important for the maintenance of cell survival after exposure to high-temperature (Nishimura et al. 2013; Nasuno et al. 2014; Liu et al. 2015). An excessive NO level in yeast generally originates from external exposure. For instance, *C. albicans*, which is the human pathogenic yeast, is exposed to a high level of NO produced by the i-NOS of macrophages for pathogen eradication (Nathan and Shiloh 2000; Tillmann et al. 2011). Under experimental conditions, excessive NO levels can be induced by the addition of exogenous NO donors, such as diethylenetriamine NONOate (DETA-NONOate) (Liu et al. 2000; Sarver and DeRisi 2005), NO-amine complex and its derivatives (Yamanaka et al. 1996; Sun et al. 2003), sodium nitroprusside (SNP) (Grossi and D'Angelo 2005), *S*-nitroso-*N*-acetyl penicillamine (SNAP) (Gelaude et al. 2015; Zhang et al. 2003), and sodium nitrite in low pH (acidified NO_2^-) (Modin et al. 2001; Stamler et al 1992). In low pH, sodium nitrite ($NaNO_2$) forms nitrous acid (HNO_2) and releases NO. Microarray analysis revealed that some genes are differentially expressed under two conditions, i.e., in the presence or absence of excessive NO (Sarver and DeRisi 2005). Thus far, there are many proteins involved in excessive NO response in yeast, including the detoxification enzymes in the GSH and Trx system, which show a similar function to mammalian cells, and as well as the yeast flavohemoglobin (FHb) (Liu et al. 2000).

The *YHB1* gene encodes the yeast FHb, which is a family of nitric oxide dioxygenase (NOD) and has been well studied for its involvement in NO detoxification (Tillmann et al. 2011). FHb protects yeast cells against excessive NO levels by converting NO into nitrate. Heme reduces NO to nitrate using oxygen, and as a consequence, ferrous ion is oxidized to ferric ion. Ferric ion is reduced back to ferrous heme by accepting an electron from NADPH facilitated by flavin (FAD) (Figure 3). Meanwhile, deletion of *YHB1* in *S. cerevisiae* causes *S*-nitrosylation of proteins and inhibition of cell growth after exposure to an NO donor, DETA-NONOate (Liu et al. 2000). In addition, it has been

reported that *YHB1* expression in response to excessive NO is modulated by the transcription factor Cta4 (Chiranand et al. 2008). A functional genomic study of *S. cerevisiae* revealed the involvement of other transcription factors related to oxidative stress or nitrosative stress response, such as Yap1 and Msn2/4 (Horan et al. 2006). The involvement of transcription factors, Fzf1p, in response to nitrosative stress suggests the existence of regulation at the transcriptional level, which alters the gene expression pattern (Sarver and DeRisi 2005). However, FHb occupies an important position as one of the major NO scavengers in yeast cells. In this study, to search for novel genes involved in NO tolerance, I took a different approach by introducing the multicopy plasmid library into *S. cerevisiae* cells (Figure 4), and using acidified NO_2^- as an inducer of excessive NO.
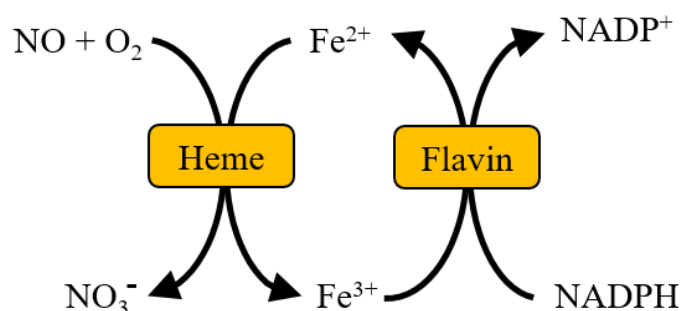
Figure 3. NO detoxification reaction by flavohemoglobin. (Adapted from Forrester et al. 2011)

FHb commonly has two domains, which are heme and flavin domain. Heme binds NO and converts NO into nitrate in the presence of oxygen. NADPH reduced ferric ion (Fe^{3+}) back into ferrous ion (Fe^{2+}) with electron transfer in the flavin domain.
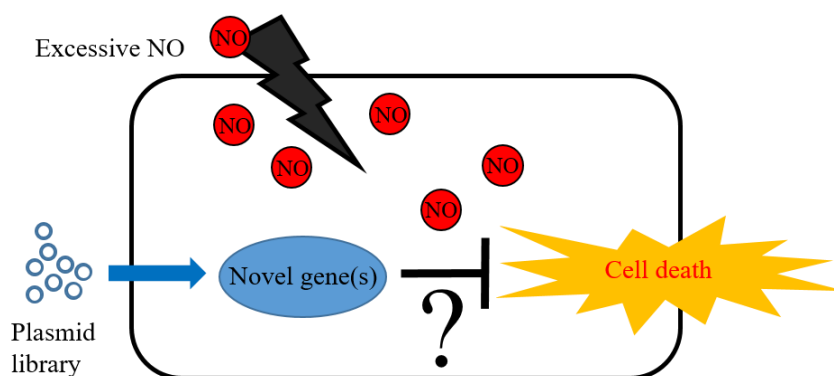
Figure 4. Schematic study model of screening process for novel genes involved in NO tolerance in *S. cerevisiae*.

1.4. Riboflavin; functions and biosynthesis

RF (7,8-dimethyl-10-ribityl-isoalloxazine) or vitamin B_2 is an essential water-soluble vitamin for humans. RF is endogenously synthesized in bacteria, yeasts, and plants. However, human cells must intake RF from food (Powers 2003, Abbas and Sibirny 2011). In *S. cerevisiae* cells, RF biosynthesis involves the roles of multiple enzymes encoded by *RIB1*, *RIB7*, *RIB2*, *RIB3*, *RIB4*, and *RIB5* (Table 2, Figure 5). Rib1p, which is guanosine triphosphate cyclohydrolase 2 (GTPCH2), catalyzes the first step of RF biosynthesis, and is the rate-limiting step of this biosynthesis (Gräwet et al. 2013). In addition, this pathway is connected with the biosynthesis of flavin mononucleotide (FMN) and flavin adenine dinucleotide (FAD), in which RF is a necessary precursor. Since FMN and FAD are essential coenzymes for flavoproteins, RF acts as an important compound to maintain cellular functions. For instance, the yeast FHb encoded by the *YHB1* gene, which plays a role in excessive NO response, also needs FAD as a cofactor (Gudipati et al. 2014).

Table 2. Biosynthesis of Riboflavin, FMN and FAD in *S. cerevisiae*

No.	Substrate	Enzyme	Coding Gene	Final Product
1.	Guanosine triphosphate (GTP)	GTP cyclohydrolase 2 (GTPCH2)	*RIB1*	DARP
2.	2,5-Diamino-6-(5-phospo-D-ribosylamino)-pyrimidin-4(3H)-one (DARP)	DARP-reductase	*RIB7*	DARIP
3.	2,5-Diamino-6-(5-phospo-D-ribitylamino)-pyrimidin-4(3H)-one (DARIP)	Deaminase	*RIB2*	ARIP
4.	Ribulose-5-phosphate (DRP)	DHBP synthase	*RIB3*	DHBP
5.	5-Amino-6-(ribitylamino)uracil (ARIP); 3,4-Dihydroxy-2-butanone-4-phosphate (DHBP)	Lumazine synthase	*RIB4*	DMRL
6.	6,7-dimethyl-8-ribityllumazine (DMRL)	Riboflavin synthase	*RIB5*	Riboflavin
7.	Riboflavin (RF)	Riboflavin kinase	*FMN1*	FMN
8.	Flavin mononucleotide (FMN)	FAD synthetase	*FAD1*	FAD

Guanosine triphosphate
(GTP)

↓ **Rib1**

2,5-Diamino-6-(5-phospo-D-ribosylamino)-pyrimidin-4(3H)-one
(DARP)

↓ Rib7

Ribulose-5-phosphate
(DRP)

2,5-Diamino-6-(5-phospo-D-ribitylamino)-pyrimidin-4(3H)-one
(DARIP)

↓ Rib3

↓ Rib2

3,4-Dihydroxy-2-butanone-4-phosphate
(DHBP)

5-Amino-6-(ribitylamino)uracil
(ARIP)

↓ Rib4

6,7-Dimethyl-8-ribityllumazine
(DMRL)

↓ Rib5

Riboflavin (RF)

↓ Fmn1

Flavin mononucleotide
(FMN)

↓ Fad1

Flavin adenine dinucleotide
(FAD)

Figure 5. The metabolic pathway of riboflavin in *S. cerevisiae*.

1.5. Research objectives of my doctoral thesis

1. To identify the gene(s) involved in NO tolerance by use of the multicopy plasmid library in *S. cerevisiae*.

2. To characterize the identified gene(s) involved in NO tolerance for elucidation of the molecular mechanism in *S. cerevisiae*.

2. MATERIALS AND METHODS

2.1. Strains and plasmids

The yeast *Saccharomyces cerevisiae* with an S288c background BY4741 (*MATa his3Δ1 leu2Δ0 met15Δ0 ura3Δ0*) was used in this study as a wild-type strain. The yeast strains used in this study are listed in Table 3.

An *Escherichia coli* DH5α strain was used for plasmid construction. For the production of recombinant proteins, *E. coli* Rosetta (DE3) strain was used. The plasmid libraries used in this study, BYP6127-6139, were obtained from the Yeast Genetic Research Center (YGRC), a National Bioresearch Project (NBRP) on yeast. The library was originated from yeast genomic DNA of *S. cerevisiae*, X2180-1A strain, which was digested by *Sau*3AI and partially fractionated using sucrose gradient. The plasmid library vector Yep51B was derived from YEp51 plasmid, which contains 2-micron replication origin, and *LEU2* marker (Akada et al. 1997). The plasmids used in this study are listed in Table 4.

The DNA fragments containing 13×Myc (13Myc) or 6×HA (6HA) tag sequence were amplified with the primers listed in Table 5 from pFA6a-13Myc-kanMX6 or pYM16 by polymerase chain reaction (PCR) respectively (Knop et al. 1999; Janke et al. 2004). Each DNA fragment was introduced to BY4741 strain to generate BY4741 RIB1-13Myc or BY4741 RIB7-6HA, expressing Rib1p fused with 13Myc or Rib7p fused with 6HA at the C-terminus, respectively.

Plasmid pRS416-CgHIS3-MET15 (Nishida et al. 2016) was used to complement the uracil, histidine and methionine auxotrophy of BY4741 strain. pAG415GPD-RIB1-13Myc used for overexpression of *RIB1* was constructed by BP and LR reaction in Gateway technology (Invitrogen). The DNA fragment amplified using the primers Rib1 (attb1) Fw and attB RIB1-13Myc-*kanMX6* Rv primers from genomic DNA of BY4741 RIB1-13Myc was introduced into plasmid pDONR221-ccdB by the BP reaction. After confirmation of the correct sequence, the LR reaction was performed using the resultant plasmid pDONR221-RIB1-13Myc and pAG415GPD-ccdB to construct pAG415GPD-RIB1-13Myc.

Plasmids pAG415GPD-RIB1-13Myc, pAG425GPD-HEK2-3HA, and

pAG425GPD-YHB1-3HA were introduced into BY4741 cells harboring plasmid pRS416-CgHIS3-MET15 to construct yeast cells overexpressing *RIB1*, *HEK2*, and *YHB1* respectively.

The DNA fragment containing the GPD promoter was amplified by using *RIB7* S1 and S4 primers from plasmid pYM-N15. The DNA fragment was introduced into BY4741 strain to construct BY4741 P_{GPD}-RIB7-6HA RIB1-13Myc. To construct the *RIB7* overexpressing cells, plasmids pRS416-CgHIS3-MET15 and pAG415GPD-ccdB were introduced into BY4741 P_{GPD}-RIB7-6HA RIB1-13Myc. Meanwhile, for the *RIB1-RIB7* co-overexpressing cells, pRS416-CgHIS3-MET15 and pAG415GPD-RIB1-13Myc were introduced into BY4741 P_{GPD}-RIB7-6HA RIB1-13Myc.

The sequence of *kanMX6* was amplified through PCR using plasmid pFA6a-*kanMX6* and serial of S1 and S2 primers from *RIB1*, *RIB7*, *RIB2*, and *RIB4*. The *kanMX6* fragment was introduced into BY4741 strain to replace the open reading frame (ORF) of *RIB1*, *RIB7*, *RIB2*, and *RIB4*. Plasmids pRS416-CgHIS3-MET15 and pAG415GPD-ccdB were introduced into yeast disruption cells to generate the *RIB* genes-disrupted cells. For a combination of knock-out (KO) cells and RIB1-OE, pAG415GPD-RIB1-13Myc was used instead of pAG415GPD-ccdB.

KO cells, Δ*grx1*, Δ*grx2*, Δ*glr1*, Δ*trx1*, Δ*trx2*, Δ*trx3*, and Δ*trr2* were originated from EUROSCARF. Deletion of the genes were confirmed by PCR using a forward primer containing approximately 20 bases start from about 500 bp upstream of each gene ORF and kanMX4R primer. Plasmids pRS416-CgHIS3-MET15 and pAG415GPD-ccdB were introduced into KO cells to generate KO cells harboring empty vector (EV) and pRS416-CgHIS3-MET15 with pAG415GPD-RIB1-13Myc were introduced into KO cells to construct KO cells overexpressing *RIB1*.

Table 3. Yeast strains used in this study

Strains	Genotype	Source or reference
BY4741	*MAT*a *his3Δ1 leu2Δ0 met15Δ0 ura3Δ0*	EUROSCARF
Δ*rib1*	BY4741 Δ*rib1::kanMX6*	In this study
Δ*rib7*	BY4741 Δ*rib7::kanMX6*	In this study
Δ*rib2*	BY4741 Δ*rib2::kanMX6*	In this study
Δ*rib4*	BY4741 Δ*rib4::kanMX6*	In this study

21

Δgrx1	BY4741 *Δgrx1::kanMX6*	EUROSCARF
Δgrx2	BY4741 *Δgrx2::kanMX6*	EUROSCARF
Δglr1	BY4741 *Δglr1::kanMX6*	EUROSCARF
Δtrx1	BY4741 *Δtrx1::kanMX6*	EUROSCARF
Δtrx2	BY4741 *Δtrx2::kanMX6*	EUROSCARF
Δtrx3	BY4741 *Δtrx3::kanMX6*	EUROSCARF
Δtrr2	BY4741 *Δtrr2::kanMX6*	EUROSCARF
Δyhb1	BY4741 *Δyhb1::kanMX6*	EUROSCARF

Table 4. Plasmids used in this study

Plasmids	Description	Source or reference
BYP6127-6139	*LEU2*, 2-micron, *GAL10*	NBRP
pRS416-CgHIS3-MET15	*URA3*, *HIS3*, *MET15*	Nishida et al. 2016
pAG425GPD-ccdB-HA	*LEU2,* 2-micron, GPD promoter, *ccdB,* 3HA*, CYC1* terminator	Invitrogen
BG1805-RIB1	*RIB1, AmpR*	Invitrogen
pDONR221-ccdB	*KanR, ccdB*	Invitrogen
pAG415GPD-ccdB	*LEU2*, GPD promoter, *ccdB, CYC1* terminator	Invitrogen
pFA6a-13Myc-kanMX6	13Myc*, kanMX6*	EUROSCARF
pDONR221-RIB1-13Myc	*KanR, RIB1*-13Myc	In this study
pAG415GPD-RIB1-13Myc	*LEU2*, GPD promoter, *RIB1*-13Myc, *CYC1* terminator	In this study
pFA6a-kanMX6	*kanMX6*	EUROSCARF
pDONR221-RIB1	*KanR, RIB1*	In this study
pDONR221-RIB1^{C148S}	*KanR, RIB1^{C148S}*	In this study
pDONR221-RIB1^{C148S}-13Myc	*KanR, RIB1^{C148S}* -13Myc	In this study
pDONR221-RIB1^{C159S}-13Myc	*KanR, RIB1^{C159S}* -13Myc	In this study
pDONR221-RIB1^{C161S}-13Myc	*KanR, RIB1^{C161S}* -13Myc	In this study
pAG415GPD-RIB1^{C148S}-13Myc	*LEU2*, GPD promoter, *RIB1^{C148S}*-13Myc, *CYC1* terminator	In this study
pAG415GPD-RIB1^{C159S}-13Myc	*LEU2*, GPD promoter, *RIB1^{C159S}*-13Myc, *CYC1* terminator	In this study
pAG415GPD-RIB1^{C161S}-13Myc	*LEU2*, GPD promoter, *RIB1^{C161S}*-13Myc, *CYC1* terminator	In this study
pET53-ccdB	*AmpR, ccdB*, 6xHis-tag, Strep-tag, T7 promoter, *LacI* promoter, T7 terminator	EUROSCARF

pET53-RIB1	*AmpR, RIB1,* 6xHis-tag, Strep-tag, T7 promoter, *LacI* promoter, T7 terminator	In this study
pET53-RIB1 [C148S]	*AmpR, RIB1* [C148S], 6xHis-tag, Strep-tag, T7 promoter, *LacI* promoter, T7 terminator	In this study
pYM16	6HA, *hphNT1*	EUROSCARF
pYM-N15	GPD promoter, *natNT2*	EUROSCARF
pDONR221-HEK2	*KanR, HEK2*	In this study
pDONR221-YHB1	*KanR, YHB1*	Lab collection
pAG425GPD-HEK2-3HA	*LEU2,* 2-micron, GPD promoter, *HEK2,* 3HA, *CYC1* terminator	In this study
pAG425GPD-YHB1-3HA	*LEU2,* 2-micron, GPD promoter, *YHB1,* 3HA, *CYC1* terminator	In this study

Table 5. Primers used in this study

Primer	Sequence (5' to 3')
F2_Library	ACTCCGTTAGGCCCTTCATT
S1_RIB1_Fw	ACAAAAAGTGGCGTACATAAAACTACAACAAACCTACAGGATGcgtacgctgcaggtcgac
S2_RIB1_Rv	AAAAGCACTATATGTACTAATAATTATGCTACACTTGTGTTTAatcgatgaattcgagctcg
S3_RIB1_Fw	TATGAACTCTGCGTTGTCATCAACATCGACGCTGGCAATAcgtacgctgcaggtcgac
S3 primer new	AACTCTGCGTTGTCATCAACATCGACGCTGGCAATAtcgtacgctgcaggtcga
S4_RIB1_Rv	TATTTGCTGCTATCCTGTTTACTGTTGTCGTAGTTATCTATGGTcatcgatgaattctctgtcg
S1 primer_RIB2	AAGAACATTAAAAAAAAAACTATCAATATTAGATTAACAAACCAATCAAAATGcgtacgctgcaggtcgac
S2 primer_RIB2	GTGGTTATTGTAGATATGATGTAAGATTACATGATAATATATATGCTAAATAGTTTAatcgatgaattcgagctcg
500bp_up_RIB2 Fw	TCCCTAGGTCCAATGCTCTA
500bp_down_RIB2 Rv	TTCCACCTCCTCTCTGTTCT
S1 primer_RIB4	AAGGAACAGTATAACGCAGTATAACGCAGTATAACGCAGTATAACGCAGTATGcgtacgctgcaggtcgac
S2 primer_RIB4	TTCTATAGTGAGTATATACATATATAGTATAGATTTCTCTGCGCTTATTTAatcgatgaattcgagctcg
500bp_up_RIB4 Fw	GTAGGGTCTACAGGAAAGCT
500bp_down_RIB4 Rv	ACGGGCAGGAGGATAATGAA
S1 primer_RIB7	ACCAACCTATTGGTAGCTTCTTTGTATTACTATCAACATTTTTAGAAGATATGcgtacgctgcaggtcgac

S2 primer_RIB7	CTAATTTCAGAAAGAAATTACACAGAAGGTGGAGT TCTAACACTATTAatcgatgaattcgagctcg
500bp_up_RIB7 Fw	GGCAGAACGAACGAAAGCAA
500bp_down_RIB7 Rv	CCTTCCGTTGGTGTAAAGAC
Rib1 (attb1) Fw	ggggacaagtttgtacaaaaaagcaggcttaATGACCATAGATAACT ACGA
Rib1 (attb2) Rv	ggggaccactttgtacaagaaagctgggtgTATTGCCAGCGTCGATG TTG
attB RIB1-13Myc-kanMX6 Rv	ggggaccactttgtacaagaaagctgggtgCTAGTGATTGATTAATT T
RIB1 599 Fw (seq)	GCATCGGGTTAGGTGAGAAA
C148S_Fw	AGTTACACCGGTGAAAACGC
C148s_Rv	TTCAGAATGGATCCGTACCAGCG
C159S_Fw	AGTGATTGTGGTGAACAATTCG
C159S_Rv	ACGGGCGCTCCATGCGTTTTC
C161S_Fw	AGTGGTGAACAATTCGATAGGG
C161S_Rv	ATCACAACGGGCGCTCCATG
RIB7 S3 primer	ATGGTGGAAGGGCATTACCGATGTGGTGCTTTGTGC GAGACTGGCCGATGACcgtacgctgca ggtcgac
RIB7 S4 primer	TAGTTTTGCAGAAATTGTGGTAAATCTTCACACAGT GGTGTCAAAGAcatcgatgaattctct gtcg
RIB1_upstr_100bp_Fw	TAGTCGGACGCTCTTGTGG
RIB1_down_100bp_Rv	ATGTTAATGCGCCAATACGC
kanMX4F	CATGGCAAAGGTAGCGTTG
kanMX4R	CCGACTCGTCCAACATCAATAC
M13_Fw	GTAAAACGACGGCCAG
M13_Rv	CAGGAAACAGCTATGAC
GRX1 500bp upstream Fw	TAGCTGTATGCGGATGATCCG
GRX2 500bp upstream Fw	CCTCTCCTGCCATATAACC
GLR1 500bp upstream Fw	GATGCTGCATGCTGCCCGTA
TRX1 500bp upstream Fw	GTTGACCCAAGACAAGTCTT
TRX2 500bp upstream Fw	CTGTGAAGAACATCCAGACT
TRX3 500bp upstream Fw	TGATGTATTGGCGGAGAATAGG
TRR2 500bp upstream Fw	TTGCGGCCAAGAGGGAAAGC
YHB1 500bp upstream Fw	AATGATAGTCTGCGCGGCAA

2.2. Medium

The yeast *S. cerevisiae* cells were cultivated in the nutrient YPD medium, which consists of 1% yeast extract, 2% peptone and 2% dextrose, and the minimal synthetic defined (SD) medium, which consists of 0.17% yeast nitrogen base without amino acid, 0.5% ammonium sulfate and 2% dextrose. The SD medium was supplemented with uracil, L-leucine, L-histidine, and L-methionine for complementing the auxotrophic markers of the parental yeast strain. The pH of SD medium was adjusted with 1 N sodium hydroxide (NaOH) at pH 5.5-6.0. The excessive NO conditions were induced by the addition of sodium nitrite ($NaNO_2$) in the acidic medium (SD medium at pH 5.5) or called acidified NO_2^- condition. The 1 M $NaNO_2$ stock was dissolved in 10 mM NaOH, aliquoted and kept frozen in -30°C. Excessive NO condition derived from NO donor, NOC-5 (Dojindo) also been used. For homologous recombination screening processes, 200 mg/l geneticin (G418), 300 mg/l hygromycin, and 100 mg/l nourseothricin were used in YPD medium. Luria-Bertani (LB) medium used for *E. coli* cultivation consists of 0.5% yeast extract, 1% tryptone, and 1% NaCl. Recombinant cells of *E. coli* were grown in LB containing 200 mg/l ampicillin, 100 mg/l kanamycin, and 35 mg/l chloramphenicol.

2.3. Yeast transformation

The yeast host cells were inoculated into 2 ml of liquid SD medium at pH 6 supplemented with leucine incubated at 30°C with agitation at 300 round per minutes (rpm) overnight. The overnight cell culture was then diluted into 40 ml SD + leucine medium and then incubated at 30°C with agitation at 140 rpm, from initial optical density at wavelength 600 nm (OD_{600}) = 0.05 to reach OD_{600} = 0.8. After the incubation, the cell culture was harvested by centrifugation. The cell pellet was then washed with mili-Q to remove the leftover medium before then being centrifuged again. The cell pellet was resuspended in 1 ml of 0.1 M lithium-acetate (Li-Ac) and then was incubated at 30°C for 1 hour. The cell suspension OD_{600} in Li-Ac solution was measured to determine OD_{600} = 10 (10^8 cells) in each tube. The cell suspension was briefly centrifuged and the supernatant was removed. About 75 µl of solution containing single-stranded DNA (ss-DNA) of salmon sperm, 1 µg of plasmid DNA, and mili-Q was added into cell pellet. After resuspending the cell pellet, 36 µl of 1 M Li-Ac and 240 µl of 50% PEG 4000

solutions were added into the tube and then mixed homogeneously. The cell suspension was incubated at 30°C for 1 hour. Afterward, 40 µl DMSO was added into the tube and directly heat-shocked at 42°C for 20 minutes. Next, the cells were spun and then re-suspended in 1 ml YPD medium. After 1-hour incubation at 30°C, the cells were spun again and then washed 2 times by using sterilized mili-Q. After washing, the cell pellet was resuspended in 1 ml mili-Q. Finally, 100 µl of culture suspension was spread on the selection medium and incubated at 30°C for 2-4 days.

2.4. Construction of the plasmids expressing the mutant *RIB1*

Amino acid substitutions of the Zn^{2+}-binding site of Rib1p at positions 148, 159, and 161 were done by point mutations (site-directed mutagenesis) in the gene that converts the cysteine base pair, TGT, into serine, AGT. An entry clone, pDONR221-RIB1-13Myc was used to construct the mutant *RIB1* genes through inverse PCR using C148S_Fw, C148s_Rv, C159S_Fw, C159S_Rv, C161S_Fw, and C161S_Rv primers. The correct sequence of each mutation in the colony was confirmed by using M13_Fw, M13_Rv, and RIB1 599 Fw primers. Next, the entry clones were combined with pAG415GPD-ccdB by the LR reaction to construct plasmids pAG415GPD-RIB1^{C148S}-13Myc, pAG415GPD-RIB1^{C159S}-13Myc, and pAG415GPD-RIB1^{C161S}-13Myc.

2.5. Intracellular NO estimation

Yeast cells were inoculated in 2 ml of SD medium at pH 5.5 for 24 hours and then diluted into 10 ml of fresh medium with initial $OD_{600} = 0.05$ and incubated for 12 hours or until the cell culture reached approximately $OD_{600} = 1$. The cell culture was added by 4-amino-5-methylamino-2',7'-difluorofluorescein diacetate (DAF-FM DA), 30 minutes before the treatment. The final concentration of DAF-FM DA was 10 µM. The cell culture was divided into treated group and untreated group in a new tube. Serial concentrations of 0.5, 1, 2, and 4 mM $NaNO_2$ or 0.5 mM NOC-5 (an NO donor) were used as excessive NO treatment and 10 mM sodium hydroxide (NaOH) was used as control. The sample was collected every 0, 1, and 2-hour incubation time. As a sample, 100 µl of cell culture was diluted 10 times with 900 µl of PBS buffer (pH 7.4). The fluorescence intensity (FL1-H) was measured by flow cytometer (BD Accuri C6) with

10,000 events (Yoshikawa et al. 2016). The relative fluorescence intensity was measured by dividing the fluorescence intensity at sampling time with the fluorescence intensity at 0-hour incubation time in percentage

2.6. Optimization of screening medium

Plasmid pAG425GPD-ccdB-HA was introduced into BY4741 strain harboring pRS416-CgHIS3-MET15 and then spread on SD plates at pH 5.5 containing various concentrations of $NaNO_2$, from 0-8 mM, and incubated at 30°C for 2-4 days. The medium in which can inhibit the cell growth completely was used as a screening medium.

2.7. Screening using the plasmid library

The multicopy plasmid library, BYP6127-6139, was introduced into BY4741 strain harboring pRS416-CgHIS3-MET15 and then spread on SD plate containing 8 mM $NaNO_2$ at pH 5.5. In these screening processes, SD plate at pH 5.5 without $NaNO_2$ was used for the calculation of transformation efficiency. For negative control, pAG425GPD-ccdB-HA (EV) was introduced into yeast host cells instead of plasmid library on SD plate containing 8 mM $NaNO_2$ at pH 5.5.

2.8. Spot test

Yeast cells were inoculated in 2 ml of SD medium at pH 5.5 for 24 hours and then diluted into 2 ml of fresh medium with initial $OD_{600} = 0.05$ and incubated until the cell culture reached $OD_{600} = 1$. The cell culture was collected as pellet, then washed by mili-Q water to remove the excess medium and resuspend in 200 μl of mili-Q water. The cell suspension was diluted with 10-fold serial dilutions, from $OD_{600} = 1$ to 10^{-4}. The diluted cell suspension was spotted as much as 3 μl on SD plates at pH 5.5. For observing the NO tolerance, 0 to 5 mM $NaNO_2$ were used as a final concentration on SD plates at pH 5.5. To complement the auxotrophic of RF synthesis, 50 mg/l of RF was added into the medium (Reihl and Stolz 2005). RF was added into medium since pre-culture, main culture, and in the agar plate. The plate was incubated at 30°C for 2-4 days. For the second screening process, 5 μl of $OD_{600} = 0.1$ cells were spotted on SD plate containing 5 mM $NaNO_2$ at pH 5.5.

2.9. Plasmid extraction from yeast

Genomic DNA of yeast clone was isolated, which would also contain plasmid DNA. The genomic DNA containing plasmid DNA was introduced into *E. coli* cells and then spread on LB medium containing ampicillin, 200 mg/l. Several colonies were picked up and were recultured in order to isolate the plasmid DNA. Because there were two kinds of plasmids in yeast cells, which are pRS416-CgHIS3-MET15 and the plasmid library (YEp51B), the plasmid DNA were confirmed by a restriction enzyme, *Eco*RI (Broach et al. 1983). After being identified, the isolated plasmid DNA library was introduced back into yeast host cells to form new clones.

2.10. DNA sequencing

Specific primer was used for amplification before the DNA sequencing. F2_sequence primer was used to amplify the DNA sequence in the plasmid library. In addition, M13_Fw and M13_Rv primers were used to amplify plasmid pDONR221 which contains ORF and ORF with point mutations. The PCR product was purified by ethanol precipitation prior to sequencing analysis using 3130*xl* Genetic Analyzer (Hitachi).

2.11. Cell viability assay

Yeast cells were inoculated in 2 ml of SD medium at pH 5.5 for 24 hours and then diluted into 20 ml of fresh medium with initial $OD_{600} = 0.05$ and incubated until the cell culture reached $OD_{600} = 1$. The cell cultures were divided into treated group and untreated group in a new tube. Serial concentrations on NOC-5 at 0.25 mM and 0.5 mM were used as excessive NO treatment whereas 10 mM NaOH, NOC-5 solvent solution, was used as a control in 1 ml of culture medium. Samples were collected every 0, 1, and 2-hour time incubation. The sample was diluted 1,000 times and was spread on YPD plate with 100 µl of diluted cell culture. YPD plate was incubated at 30°C for 1-2 days. The colony formation was counted using ImageJ. The relative cell viability was measured as the percentage of colony number under stress conditions divided by the colony number without stress conditions in each cell.

2.12. Protein extraction

The yeast cell pellet was homogenized in 0.3 M NaOH for 10 minutes (Matsuo et al. 2006) and was spun to collect the lysate. Next, the lysate was resuspended in SDS-sample buffer and boiled at 95°C for 3 minutes. The supernatant was collected after centrifugation and used for protein analysis, SDS-PAGE or kept at -30°C.

2.13. Western blot analysis

For SDS-polyacrylamide gel electrophoresis (SDS-PAGE), 5-10 µg of total protein was loaded into 10% of SDS-polyacrylamide gel. After electrophoresis, the protein in the gel was transferred into a polyvinylidene difluoride (PVDF) membrane by using a wet transfer method. Protein blot was blocked by 5% skim milk in Tris buffer saline containing 0.3% tween (TBST) and was incubated overnight at 4°C. After washing with TBST, the membrane was incubated with anti-hemagglutinin (HA, Santa Cruz Biotechnology), anti-glyceraldehyde-3-phosphate dehydrogenase (GAPDH), anti-PGK1, or anti-Myc antibodies for 1 hour to overnight incubation at 4°C. Following the next washing in TBST, the membrane was incubated in HRP-conjugated anti-rabbit or anti-mouse secondary antibodies. The protein band was visualized by using ECL Western blotting substrate which detected by LAS-4000 (GE/Fujifilm).

2.14. Expression and purification of the recombinant Rib1p

To produce Rib1p, *E. coli* Rosetta cells were transformed with plasmid pET53-RIB1. Rosetta cells modified from *E. coli* B21 cells enhance the expression of eukaryotic proteins which codon rarely used in *E coli*. It will supply rare tRNAs, such as AGG, AGA, AUA, CUA, CCC, and GGA. Recombinant *E. coli* cells were inoculated in 2 ml of LB medium containing 35 g/l chloramphenicol and 200 mg/l ampicillin. The culture was incubated for 12-16 hours at 30°C, 300 rpm in a tube. Then, 1/1000 of culture was inoculated into 100 ml of fresh medium and incubated for 6-7 hours at 30°C, with agitation at 140 rpm in a flask. Before induction with isopropyl β-D-1-thiogalactopyranoside (IPTG), the cell culture was pre-incubated in shaker incubator with 250 rpm speed at 18°C. After 30 minutes, 1 mM IPTG and 1% glucose were added into the flask. The cell culture next was incubated for 16-20 hours for Rib1p production. At

the end of incubation, the cell pellet was collected and kept at -80°C. For protein extraction, the pellet from 50 ml culture was resuspended and was lysed by sonication in 5 ml of lysis buffer containing 50 mM Tris-HCl (Tris buffer with hydrochloric acid) at pH 8.0, and 500 mM sodium chloride (NaCl). The suspension was spun at 5,000 rpm for 10 minutes to collect cell lysate. Afterward, the supernatant was filtered by using a 0.45 μm membrane filter to remove remaining cell debris. Recombinant Rib1p (rRib1p) was purified by Ni-NTA agarose using 50 mM imidazole as washing buffer and 500 mM imidazole as elution buffer. The eluate, which contains Rib1p, was concentrated using 10-kDa Amicon ultra centrifugal filter at 15,000 rpm for 15 minutes. Next, the buffer was exchanged with 450 μl desalting buffer (exchanged buffer) containing 50 mM Tris-HCl (pH 8.0), 1 mM Tris-carboxy ethyl phosphine (TCEP), and 10% glycerol for 3 times. The concentrated eluate was diluted into 100-400 μl as desalted lysate. The desalted lysate was kept at -30°C. SDS-PAGE and Coomassie brilliant blue (CBB) staining were performed to observe the protein purity. The desalted lysate solution was then used as the Rib1p stock for *in vitro* assays.

2.15. Rib1p enzymatic activity measurement

To measure the DARP content, a reaction was made between 25 μl desalted lysate (rRib1p) with 10 μl of 5x RIB1 assay buffer (500 mM Tris-HCl (pH 8.8), 25 mM MgCl$_2$, and 25 mM DTT), 5 μl of 10 mM GTP and 10 μl of mili-Q with a total volume of 50 μl. The solution was incubated for 30 minutes at 37°C and was terminated by adding 2.5 μl of 0.5 mM EDTA (pH 8.0). For derivatization of DARP, as the main product, into 6,7-dimethylpterin the same volume (50 μl) of derivatization reagents (1% v/v diacetyl and 15% w/v trichloroacetic acid (TCA)) were added to the mixture. DARP will react with diacetyl to form 6,7-dimethylpterin. The sample was cleared by centrifugation at 3,000 g for 10 minutes at 4°C. The DARP derivate was analyzed by fluorescence spectrophotometer (F-7000, Hitachi) at excitation wavelength 330 nm (λ_{Ex} = 330 nm) and an emission wavelength of 435 nm (λ_{Em} = 435 nm) (Yurgel et al. 2014). A standard curve was made by measuring the various concentration of 6,7-dimethylpterin in 0.5 N HCl (0-50 μM).

2.16. Preparation of the DARP-containing solution

To prepare DARP-containing solution, 50 µl of the desalted lysate (rRib1p) with 40 µl of 5x RIB1 assay buffer, 10 µl of 10 mM GTP, and 100 µl of mili-Q with a total volume of 200 µl. The solution was incubated for 2 hours at 37°C and the protein was denatured by boiling at 95°C for 5 minutes. The supernatant was cleared by centrifugation at 15,000 rpm for 20 minutes at 4°C. The supernatant was collected and moved into a new tube. DARP concentration was measured with the same method as mentioned above.

2.17. *In vitro* NO quenching assay

To measure the fluorescence intensity of DAF-FM-T, 345 µl of mili-Q, 100 µl of 5x RIB1 assay buffer (pH 7.4), and 5 µl of 0.7 mM DAF-FM were mixed, then added with 25 µl of each sample solution and 25 µl of 2 mM NOC-5, respectively. The fluorescence intensity was analyzed by fluorescence spectrophotometer at $\lambda_{Ex} = 500$ nm and at $\lambda_{Em} = 515$ nm for 30 minutes. The samples stock of DARP moiety analog (DARPM) which is 2,4,5-triamino-6-hydroxy-pyrimidine sulfate hydrate was dissolved in mili-Q water. The fluorescence intensity represents the NO level. The baseline of the fluorescence intensity at 0 minutes was normalized at a zero level.

2.18. Rib1p expression level measurement

To measure the Rib1p expression level under excessive NO, *S. cerevisiae* BY4741 RIB1-13Myc pRS416Cg-HIS3-MET15 harboring pAG415GPD-ccdB cells were pre-cultured in 2 ml SD medium at pH 5.5 and then inoculated in 20 ml SD medium at pH 5.5 with initial $OD_{600} = 0.05$. Cell culture was incubated at 30°C with agitation at 140 rpm. After reach $OD_{600} = 1$, cell culture was dispensed into 2 ml and treated under excessive NO level in SD medium containing 5 mM NOC-5 and incubated for 2 hours at 30°C with agitation at 300 rpm. The sample was collected every 1 hour for detection of Rib1-13Myc by Western blot analysis.

3. RESULTS

3.1. Confirmation of NO generation from acidified NO_2^- condition

Previous study showed that $NaNO_2$ is protonated and then reduced to NO spontaneously under acidic conditions (Modin et al. 2001; Shiva 2013). This condition can induce the excessive NO levels that cause the pathophysiological conditions. Therefore, $NaNO_2$ was used under acidic conditions (acidified NO_2^-) for the screening of genes involved in NO tolerance. To investigate whether acidified NO_2^- condition could generate NO, I observed the intracellular NO level in cells by incubating WT cells harboring EV with DAF-FM DA, followed by $NaNO_2$ at pH 5.5. DAF-FM is an NO probe that specifically reacts with NO and multiplies the fluorescence intensity, which can be detected and measured by flow cytometry (FCM). The fluorescence intensity represents the NO level. Results showed a clear elevation of intracellular fluorescence in a dose- and time-dependent manner (Figure 6), indicating that the acidified NO_2^- condition generates NO in yeast cells.
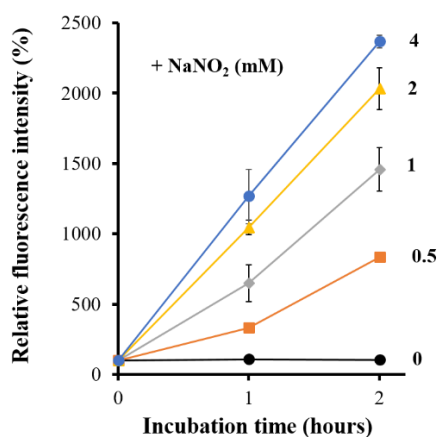

Figure 6. Relative NO level of yeast WT cells under acidified NO_2^- conditions.
Intracellular NO level measurement of *S. cerevisiae* BY4741 harboring plasmid pRS416-CgHIS3-MET15 and pAG415GPD-ccdB (EV) cells. Approximately, $OD_{600} = 1$ cells were dispensed into 1 ml culture volume and 10 μM DAF-FM DA (NO probe) was added 30 minutes before the addition of $NaNO_2$. Afterward, the cells were incubated in SD medium containing 0, 1, 2, and 4 mM $NaNO_2$ at pH 5.5 for 2 hours at 30°C with 300 rpm agitation. The relative fluorescence intensity was measured by dividing the fluorescence intensity at sampling time with the fluorescence intensity at 0-hour incubation time in percentage. Blue line indicates 4 mM $NaNO_2$; yellow line indicates 2 mM $NaNO_2$; grey line indicates 1 mM $NaNO_2$; orange line indicates 0.5 mM; black line indicates 0 mM $NaNO_2$. Data are shown in mean ± standard deviation (s.d) of triplicate experiments.

3.2. Optimization of NaNO$_2$ concentration for gene screening

To isolate the genes involved in NO tolerance, a screening medium was needed for plasmid library transformation. To determine the optimal concentration of excessive NO derived from acidified NO$_2^-$ for the screening medium, yeast cells harboring pRS416-CgHIS3-MET15 and pAG425GPD-ccdB-HA (EV) were spread on SD plates containing various concentrations of NaNO$_2$ at pH 5.5. I then examined the colony formation rate of WT cells harboring EV. I found that the number of colonies gradually decreased as acidified NO$_2^-$ concentrations increased. Finally, no colony formation was observed on SD plate containing 8 mM NaNO$_2$ at pH 5.5 (Figure 7). From these results, SD plate containing 8 mM NaNO$_2$ at pH 5.5, which generates excessive NO, was selected as the screening medium.
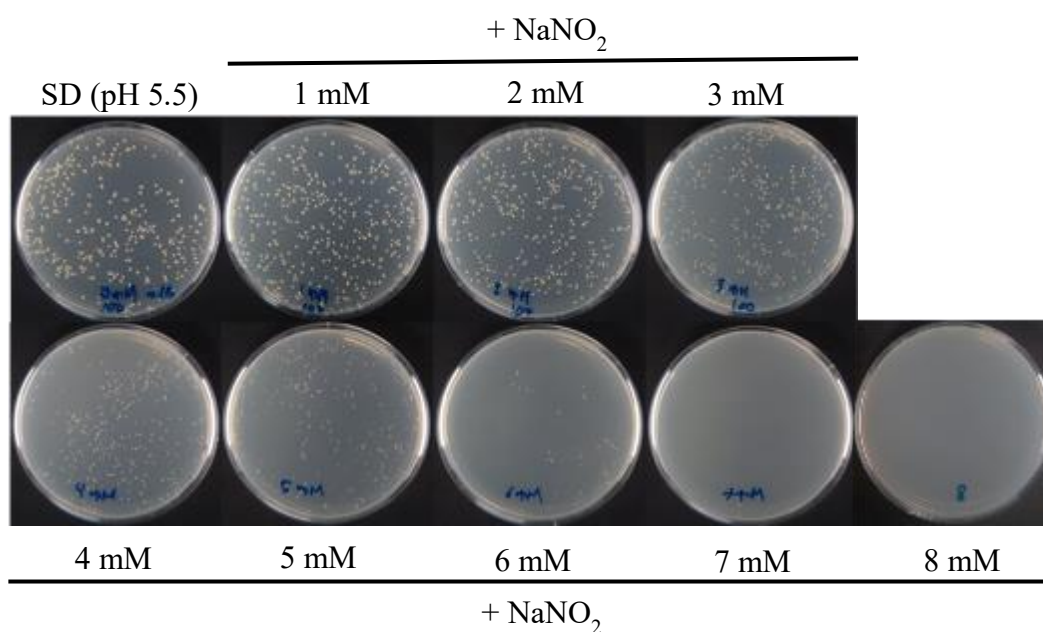

Figure 7. Optimization of the screening medium for the gene(s) involved in NO tolerance.

Plasmid pAG425GPD-ccdB-HA (EV) was introduced into *S. cerevisiae* strain BY4741 harboring pRS416-CgHIS3-MET15 and the transformant cells were spread on SD plates containing 0 to 8 mM NaNO$_2$ at pH 5.5.

3.3. Effect of yeast flavohemoglobin on acidified NO_2^- tolerance

It is known that Yhb1p is involved in the NO tolerance response by reducing NO into nitrate (Forrester et al 2011; Tillmann et al. 2011). Based on this, I tested the *YHB1* gene as a control for the screening processes of genes involved in NO tolerance. I constructed both *yhb1*-deleted cells (Δ*yhb1*) and *YHB1*-overexpression cells (YHB1-OE). I found that Δ*yhb1* cells were more sensitive than WT cells under acidified NO_2^- condition, and could be used as a negative control (Figure 8A). On the other hand, the expression level of Yhb1p was confirmed by Western blot analysis (Figure 8B), but YHB1-OE cells did not confer acidified NO_2^- tolerance, and showed the same degree of sensitivity as WT cells harboring EV (Figure 8C). This unexpected phenotype might be caused by *YHB1* overexpression, leading to the failure of the functional expression of flavohemoglobin (Tillmann et al. 2011). These results indicated that the YHB1-OE cells constructed in this study could not be used as a positive control for screening the genes involved in NO tolerance.
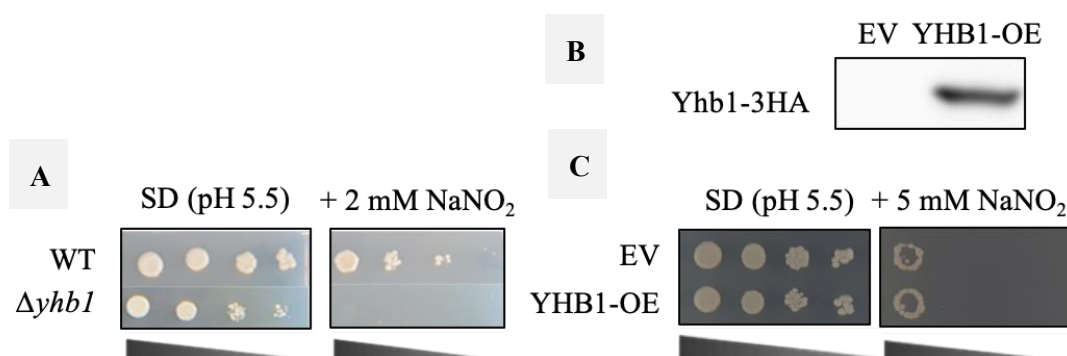

Figure 8. Yeast flavohemoglobin as a control for the genes screening.
A. Spot test of *S. cerevisiae* BY4741 WT and Δ*yhb1* harboring plasmid pRS416-CgHIS3-MET15 pAG425GPD-ccdB-3HA (EV) cells on acidified NO_2^- condition. Approximately, $OD_{600} = 1$ cells were 10-fold serially diluted to 10^{-3}, spotted on SD plate at pH 5.5 (control), and SD plate containing 2 mM $NaNO_2$ at pH 5.5, and incubated at 30°C for 2-4 days. **B.** Western blot of *S. cerevisiae* BY4741 pRS416-CgHIS3-MET15 harboring plasmid pAG425GPD-ccdB-3HA (EV) and pAG425GPD-YHB1-3HA (YHB1-OE) cells. Each lane was loaded by 10 μg of protein. **C.** Spot test of cells mentioned above on acidified NO_2^- condition. Approximately, $OD_{600} = 1$ cells were 10-fold serially diluted to 10^{-3}, spotted on SD plate at pH 5.5 (control), and SD plate containing 5 mM $NaNO_2$ at pH 5.5, and incubated at 30°C for 2-4 days.

3.4. Identification of novel genes involved in acidified NO_2^- tolerance

As the first screening, *S. cerevisiae* transformants harboring the plasmid library were spread on SD plate containing 8 mM $NaNO_2$ at pH 5.5, and the colonies with faster growth were selected. Almost 400 clones were selected with this screening process from more than 160,000 independent colonies (Figure 9).
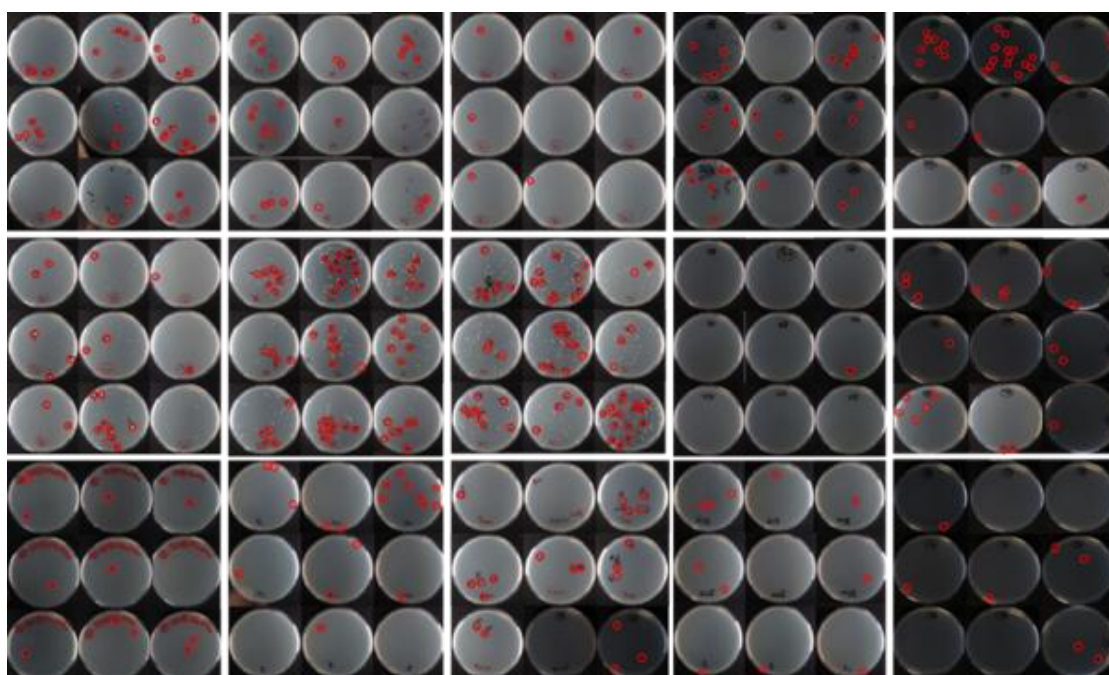

Figure 9. Colony selection after yeast transformation with the plasmid library.

Multicopy plasmid library was introduced into *S. cerevisiae* strain BY4741 harboring pRS416-CgHIS3-MET15 and then spread on SD plate containing 8 mM $NaNO_2$ at pH 5.5 and incubated at 30°C for 2-4 days. Red circles indicate colonies that were selected and were transferred into a new SD plate at pH 5.5.

For the second screening, a spot assay was conducted to examine the growth speed of the candidates isolated from the first screening. Here, about 30 clones were selected exhibiting faster growth than the cell harboring the EV on SD plate containing 5 mM NaNO$_2$ at pH 5.5 (Figure 10).
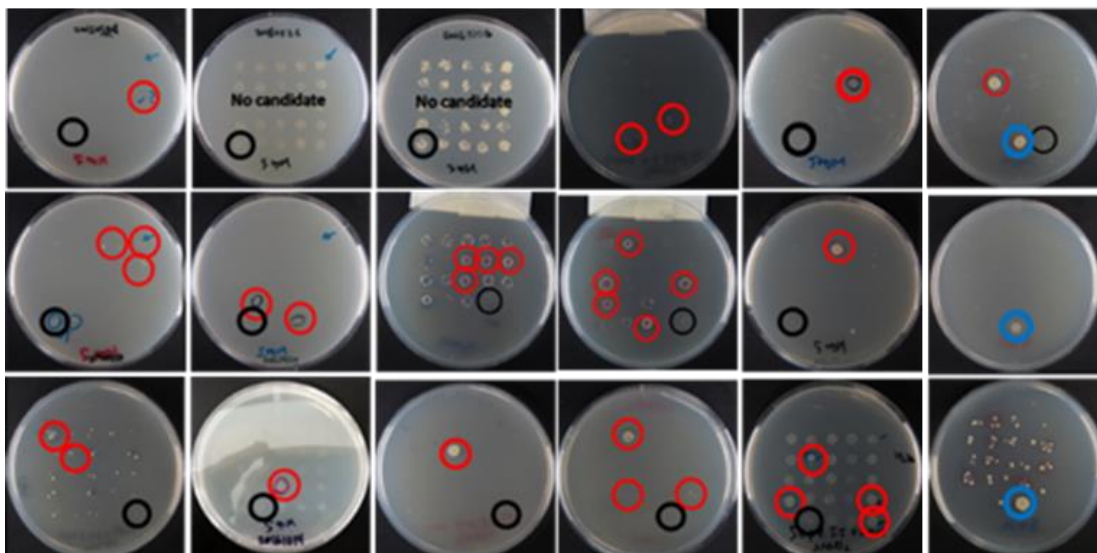

Figure 10. Colony selection based on the speed of cell growth.

Single spot test of several clones from the first screening on acidified NO$_2^-$ condition. Approximately, OD$_{600}$ = 1 cells were diluted into OD$_{600}$ = 0.1, spotted on SD plate containing 5 mM NaNO$_2$ at pH 5.5, and then incubated at 30°C for 2 days. The red circles indicate the clones, which grow fast. Black circles indicate WT cells as control and the blue circles indicate the positive control (the positive clone from earlier screening process).

For the third screening, the acidified NO_2^- tolerance of 30 candidates was analyzed by spot test with serial dilution on SD plate containing 5 mM $NaNO_2$ at pH 5.5. Figure 11 shows how candidates with higher acidified NO_2^- tolerance were selected.
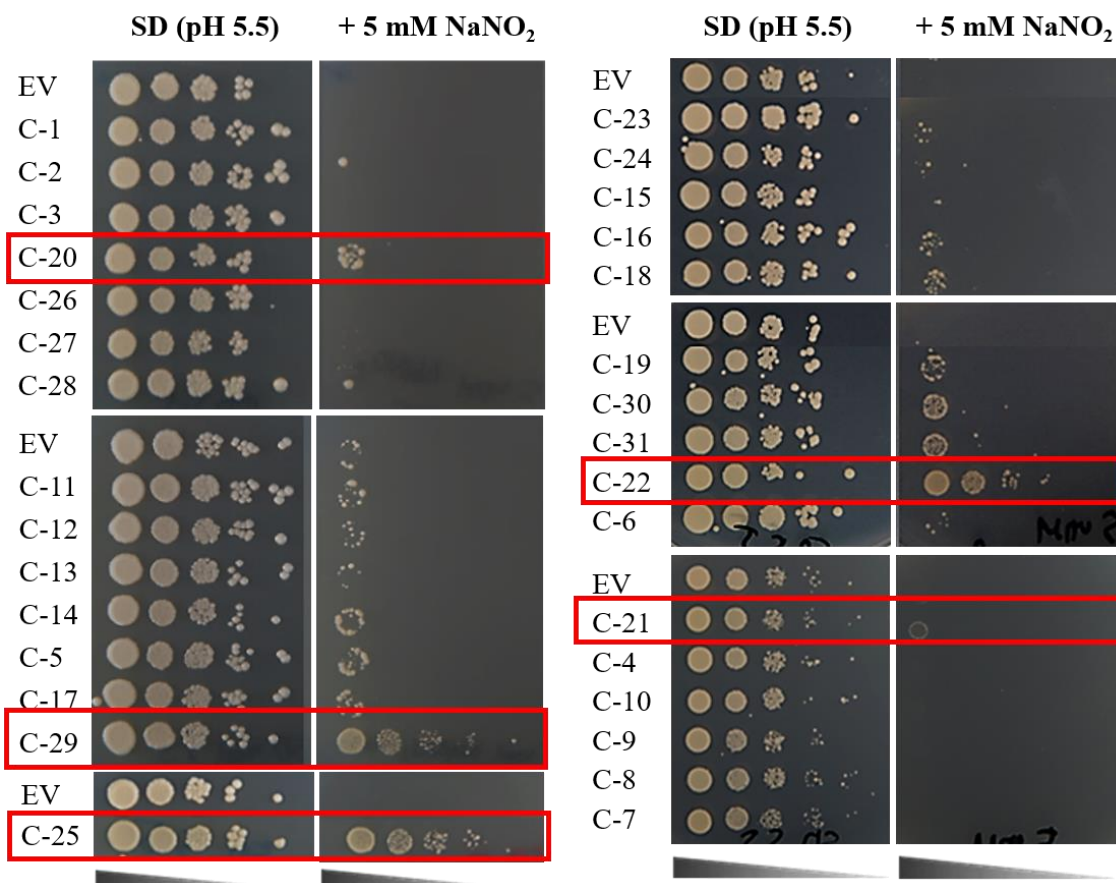

Figure 11. Serial dilution spot test of candidate clones confers the acidified NO_2^- tolerance.

Spot test of several clones from the second screening on acidified NO_2^- condition. Approximately, $OD_{600} = 1$ cells were 10-fold serially diluted to 10^{-4}, spotted on SD plate at pH 5.5 (control), and SD plate containing 5 mM $NaNO_2$ at pH 5.5, and then incubated at 30°C for 2-4 days. Red boxes indicate the clones, which showed more tolerance compared to WT harboring EV and the other clones.

To confirm whether acidified NO_2^- tolerance depends on the plasmid rather than the mutation that might have occurred in the genome, a plasmid dependency test was performed. The acidified NO_2^- tolerance of cells transformed with the plasmid library was extracted from each candidate and analyzed by spot test (Figure 12). Results suggested that four kinds of plasmids isolated from the candidate clones conferred acidified NO_2^- tolerance in yeast cells.
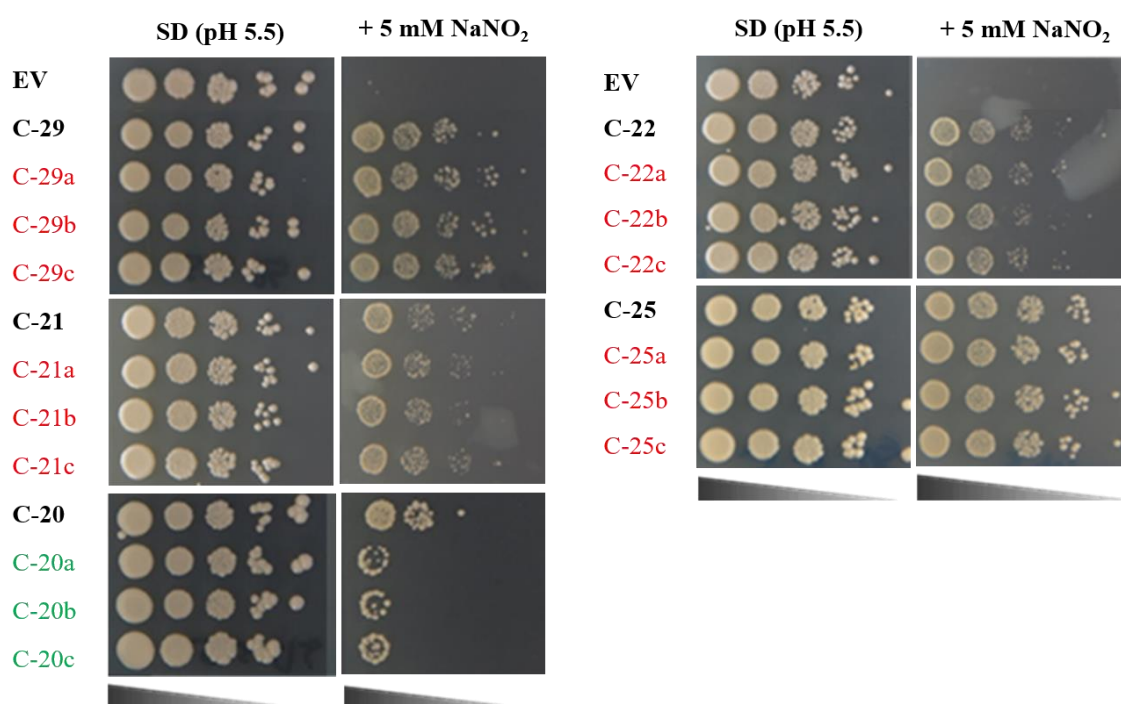

Figure 12. The plasmid dependency test of 5 candidate clones.

Spot test of new yeast clones BY4741 pRS416-CgHIS3-MET15 harboring isolated plasmid DNA library from the original yeast clones and being compared with the original clones on acidified NO_2^- condition. Approximately, $OD_{600} = 1$ cells were 10-fold serially diluted to 10^{-4} and were spotted on SD plate at pH 5.5 (control), and SD plate containing 5 mM $NaNO_2$ at pH 5.5, and incubated at 30°C for 2-4 days. Black letters indicate WT cells harboring EV and original clones, red letters indicate new clones, which are passed the plasmid dependency test, and the green letters indicate new clones, which are failed the plasmid dependency test.

The DNA sequencing of these four plasmids were determined, and it was revealed that all candidate plasmids harbored the *RIB1* gene. In addition, two candidate plasmids also contained the *HEK2* gene sequence (Figure 13), suggesting that the *RIB1* and/or *HEK2* gene confer acidified NO_2^- tolerance in yeast cells.
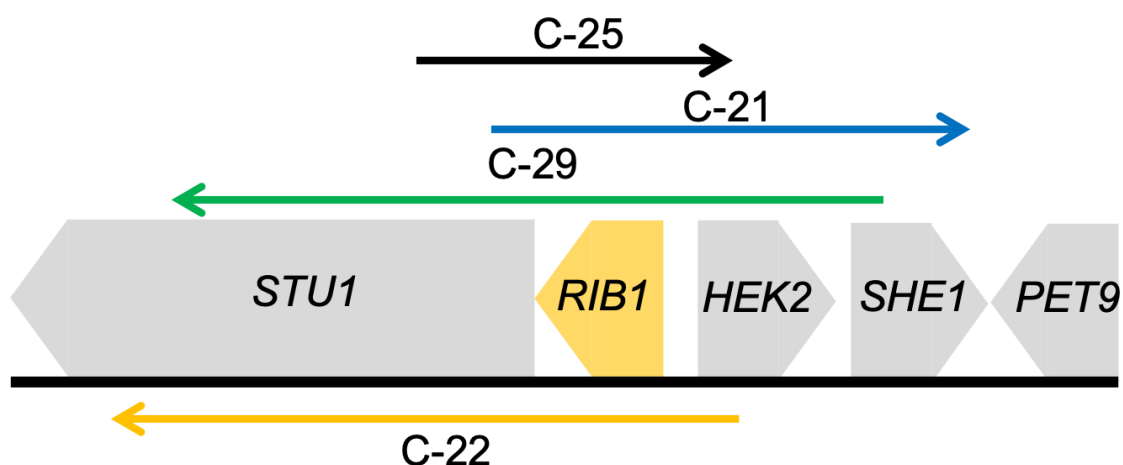

Figure 13. Genes harbored in plasmids from 4 candidate clones.

Blue line: candidate number 21 (C-21) inserted DNA fragment length is about 4.7 kilobase pair (kbp); yellow line: C-22 inserted DNA fragment length is about 6.4 kbp; black line: C-25 inserted DNA fragment length is about 3.2 kbp; green line: C-29 inserted DNA fragment length is about 7.4 kbp. All candidates are harboring *RIB1* gene. *RIB1* gene is located in chromosome II at 158656-159693 of S288c strain (parental yeast of X2180-1A). *HEK2* gene also harbored in C-21 and C-29. *HEK2* gene is located in chromosome II at 160184-161329.

To investigate the involvement of *RIB1* and *HEK2* in NO tolerance induced by acidified NO_2^- condition, *RIB1*-overexpressing (RIB1-OE) and *HEK2*-overexpressing (HEK2-OE) cells were constructed and examined under acidified NO_2^- condition. Expression of Rib1p and Hek2p was confirmed by Western blot analyses (Figures 14A and 15A). It was shown that RIB1-OE cells were more tolerant of acidified NO_2^- condition than WT cells harboring EV as controls (Figure 14B). On the other hand, HEK2-OE cells did not show higher tolerance to acidified NO_2^- condition compared to controls (Figure 15B). This suggested that *RIB1* is involved in NO tolerance induced by acidified NO_2^- condition in *S. cerevisiae*, but *HEK2* is not.
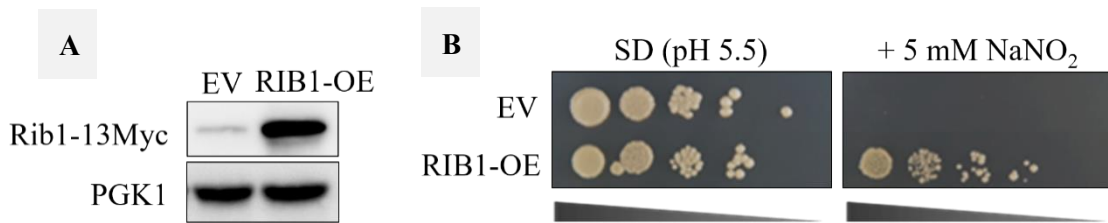

Figure 14. Overexpression of *RIB1* confers the acidified NO_2^- tolerance on *S. cerevisiae*.

A. Western blot of *S. cerevisiae* BY4741 RIB1-13myc pRS416-CgHIS3-MET15 harboring plasmid pAG415GPD-ccdB (EV) and pAG415GPD-RIB1-13myc (RIB1-OE) cells. **B.** Spot test of the cells mentioned above on acidified NO_2^- condition. Approximately, $OD_{600} = 1$ cells were 10-fold serially diluted to 10^{-4}, spotted on SD plate at pH 5.5 (control), and SD plate containing 5 mM $NaNO_2$ at pH 5.5, and incubated at 30°C for 2-4 days.

Figure 15. Overexpression of *HEK2* does not confer the acidified NO_2^- tolerance on *S. cerevisiae*.

A. Western blot of *S. cerevisiae* BY4741 pRS416-CgHIS3-MET15 harboring plasmid pAG425GPD-ccdB-3HA (EV) and pAG425GPD-HEK2-3HA (HEK2-OE) cells. Each lane was loaded by 10 μg of protein. **B.** Spot test of the cells mentioned above on acidified NO_2^- condition. Approximately, $OD_{600} = 1$ cells were 10-fold serially diluted 10^{-4}, spotted on SD plate at pH 5.5 (control), and SD plate containing 3 mM $NaNO_2$ at pH 5.5, and incubated at 30°C for 2-4 days.

To further investigate the involvement of *RIB1* in NO tolerance, RIB1-OE cells were treated under excessive NO conditions derived from a specific NO donor, NOC-5, in a liquid SD medium at pH 5.5, and cell viability was measured. NOC-5 is a specific NO donor that releases NO in a short time (Yamanaka et al. 1996). NOC-5 reacts with DAF-FM to form DAF-FM triazole, which increases its fluorescence intensity. As shown in Figure 16, the relative cell viability in RIB-OE cells was significantly higher than that of WT cells harboring EV after treatment with 0.5 mM NOC-5. This data suggests that overexpression of *RIB1* confers NO tolerance on yeast cells.
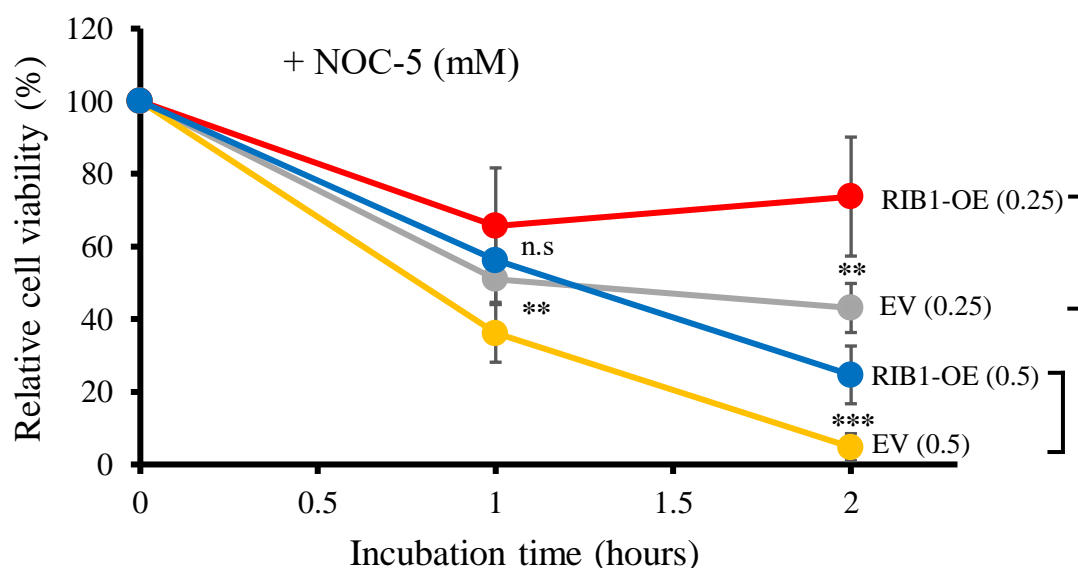

Figure 16. Overexpression of *RIB1* increases cell viability rate under excessive NO conditions induced by NO donor, NOC-5.

S. cerevisiae BY4741 RIB1-13myc pRS416-CgHIS3-MET15 harboring plasmid pAG415GPD-ccdB (EV) and pAG415GPD-RIB1-13myc (RIB1-OE) cells were treated in 1 ml SD medium containing 0.25 mM and 0.5 mM NOC-5 at pH 5.5 and were incubated for 1 hour and 2 hours at 30°C with 300 rpm agitation. The relative cell viability was measured by dividing the colony number under stress conditions with the colony number without stress condition in each cell in percentage. Data are shown in mean ± s.d of three independent experiments. Asterisks indicate significant value of student t-test; **$p<0.01$; ***$p<0.001$, and n.s indicates not significant.

3.5. Riboflavin not involved in *RIB1*-dependent acidified NO_2^- tolerance

The *RIB1* gene encodes GTP cyclohydrolase II (GTPCH2), an enzyme involved in the first step of RF biosynthesis. There are no reports regarding the involvement of GTPCH2 in NO tolerance in yeast cells. Moreover, the effect of *RIB1* might be associated with its role in the RF biosynthesis pathway. In this pathway, GTPCH2 or Rib1p converts GTP into the Rib1p reaction product called DARP (Figure 5 and Table 2), which is then modified by other enzymes encoded by other *RIB* genes, to create RF as an end product. RF is an important precursor of FMN and FAD, which are coenzymes for many flavin proteins (Abbas and Sibirny 2011), including yeast flavohemoglobin (FHb) (Gudipati et al. 2014). Flavohemoglobins are involved in NO tolerance by reducing NO into nitrate (Tillmann et al. 2011). Therefore, I investgated whether RF is involved in the acidified NO_2^- tolerance of yeast cells.

To determine whether RF could promote NO tolerance, I constructed *rib1*-deleted cells (Δ*rib1*). The expression of Rib1p was confirmed by Western blot analysis (Figure 17A). The addition of RF as a supplemental reagent in the medium is necessary for Δ*rib1* cells to grow. As shown in Figure 17B, Δ*rib1* cells could not grow on normal SD medium, but grew well on SD medium with RF supplementation, indicating the incorporation of RF into yeast cells. However, when RF was supplemented into the medium, both Δ*rib1* and control cells did not exhibit acidified NO_2^- tolerance. In addition, Δ*rib1* cells were more sensitive to the acidified NO_2^- condition compared to controls. These results indicate that RF did not confer NO tolerance under acidified NO_2^- conditions on *S. cerevisiae*.
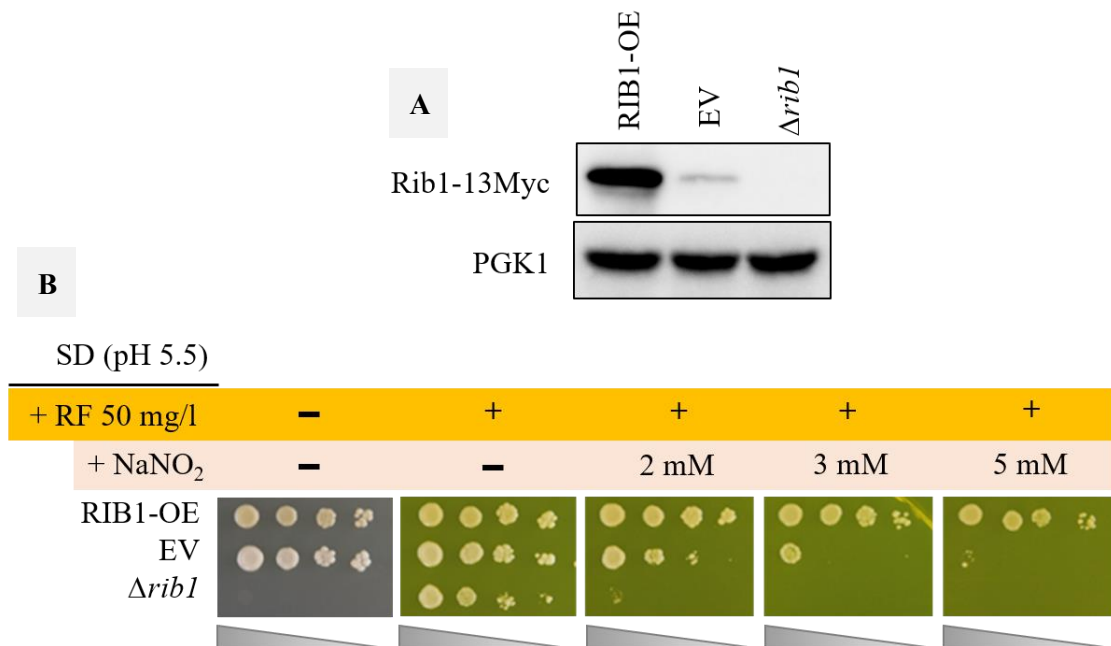
Figure 17. Riboflavin was not involved in acidified NO$_2^-$ tolerance.
A. Western blot of *S. cerevisiae* BY4741 RIB1-13myc pRS416-CgHIS3-MET15 harboring plasmid pAG415GPD-RIB1-13myc (RIB1-OE), pAG415GPD-ccdB (EV) and BY4741 Δ*rib1* pRS416-CgHIS3-MET15 harboring plasmid pAG415GPD-ccdB cells. **B.** Spot test of cells mentioned above on acidified NO$_2^-$ condition. Approximately, OD$_{600}$ = 1 cells were 10-fold serially diluted to 10^{-3}, spotted on SD plate at pH 5.5 (control), and SD plates containing 0, 2, 3, and 5 mM NaNO$_2$ at pH 5.5 with 50 mg/l riboflavin (RF), and incubated at 30°C for 2-4 days.

3.6. *RIB1*-dependent acidified NO$_2^-$ tolerance not associated with denitrosylation enzymes

The Trx system is known for controlling *S*-nitrosylation, a reaction between NO and cysteine residues in the protein (Benhar et al. 2009; Sengupta and Holmgren 2012). Through transnitrosylation, Trx removes NO from *S*-nitrosothiols. Moreover, the Rib1 protein has seven cysteine residues in its molecule, which can be targeted by *S*-nitrosylation and then neutralized by denitrosylation enzymes such as Trx or glutaredoxin (Grx). To investigate whether Rib1p has any interaction with the Trx and Grx systems, I constructed the denitrosylation enzyme gene-disrupted cells harboring either EV or the RIB1-OE plasmid (Figure 18A). The results showed that all cells, including WT and all disruptant cells, could grow well on normal SD medium. However, under the acidified

NO_2^- condition, cell growth was inhibited. The RIB1-OE could promote cell tolerance under acidified NO_2^- condition (Figure 18B). Interestingly, the RIB1-OE enhanced stress tolerance in all of the disruptant cells to the same degree as the WT cells. This implied that the effect of Rib1p in acidified NO_2^- condition was independent from the Trx or Grx systems.
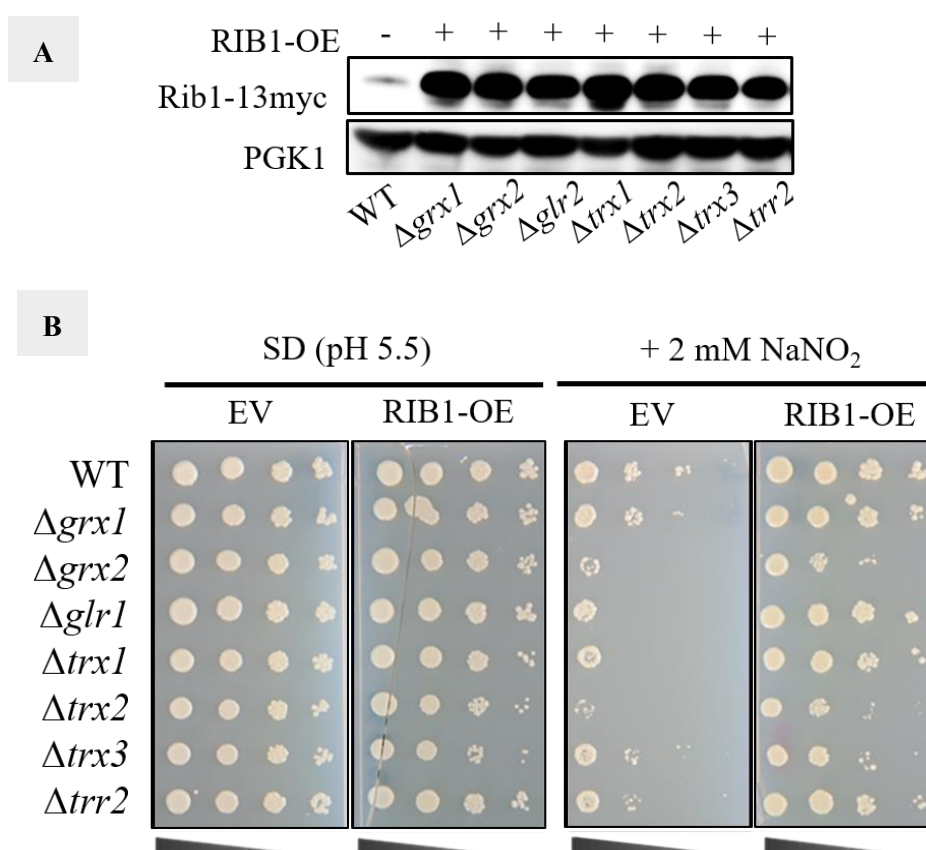

Figure 18. The role of *RIB1* overexpression in acidified NO_2^- condition response does not associate with the activities of denitrosylation enzymes.
A. Western blot of *S. cerevisiae* BY4741 RIB1-13myc pRS416-CgHIS3-MET15, BY4741 Δ*grx1*, Δ*grx2*, Δ*glr1*, Δ*trx1*, Δ*trx2*, Δ*trx3*, Δ*trr2* pRS416-CgHIS3-MET15 harboring pAG415GPD-RIB1-13myc (RIB1-OE) cells. **B.** Spot test of *S. cerevisiae* BY4741 WT, Δ*grx1*, Δ*grx2*, Δ*glr1*, Δ*trx1*, Δ*trx2*, Δ*trx3*, Δ*trr2* pRS416-CgHIS3-MET15 harboring plasmid pAG415GPD-ccdB (EV) or pAG415GPD-RIB1-13myc (RIB1-OE) cells on acidified NO_2^- condition. Approximately, $OD_{600} = 1$ cells were 10-fold serially diluted to 10^{-3}, spotted on SD plate at pH 5.5 (control) and SD plate containing 2 mM $NaNO_2$ at pH 5.5, and incubated at 30°C for 2-4 days.

3.7. Acidified NO_2^- tolerance requires the enzymatic activity of Rib1p

The experimental data suggested that the *RIB1*-dependent NO tolerance mechanism is not associated with RF or denitrosylation enzymes, which are involved in the NO tolerance mechanism. Therefore, I next investigated whether the enzymatic activity of Rib1p itself was associated with NO tolerance under acidified NO_2^- conditions. To accomplish this, I constructed *RIB1* mutants with amino acid substitutions at the Zn^{2+}-binding sites by site-directed mutagenesis. The Zn^{2+}-binding sites of this enzyme are important for its catalytic activity in modifying GTP by hydrolyzing the imidazole ring and releasing formate. Zinc binds to the three cysteine residues, which are conserved in many organisms (Kaiser et al. 2002). As the Rib1 protein possesses three Zn^{2+}-binding sites, I constructed three different mutants, harboring a different amino acid at positions 148, 159, and 161 (Figure 19A). As shown in Figure 19B, the WT and variants of Rib1p were expressed at a similar level in the host cells. However, only cells overexpressing WT Rib1p could survive under acidified NO_2^- conditions; no mutants could promote cell survival under these conditions (Figure 19C). This suggests that the catalytic activity of Rib1p is important for *RIB1*-dependent NO tolerance.
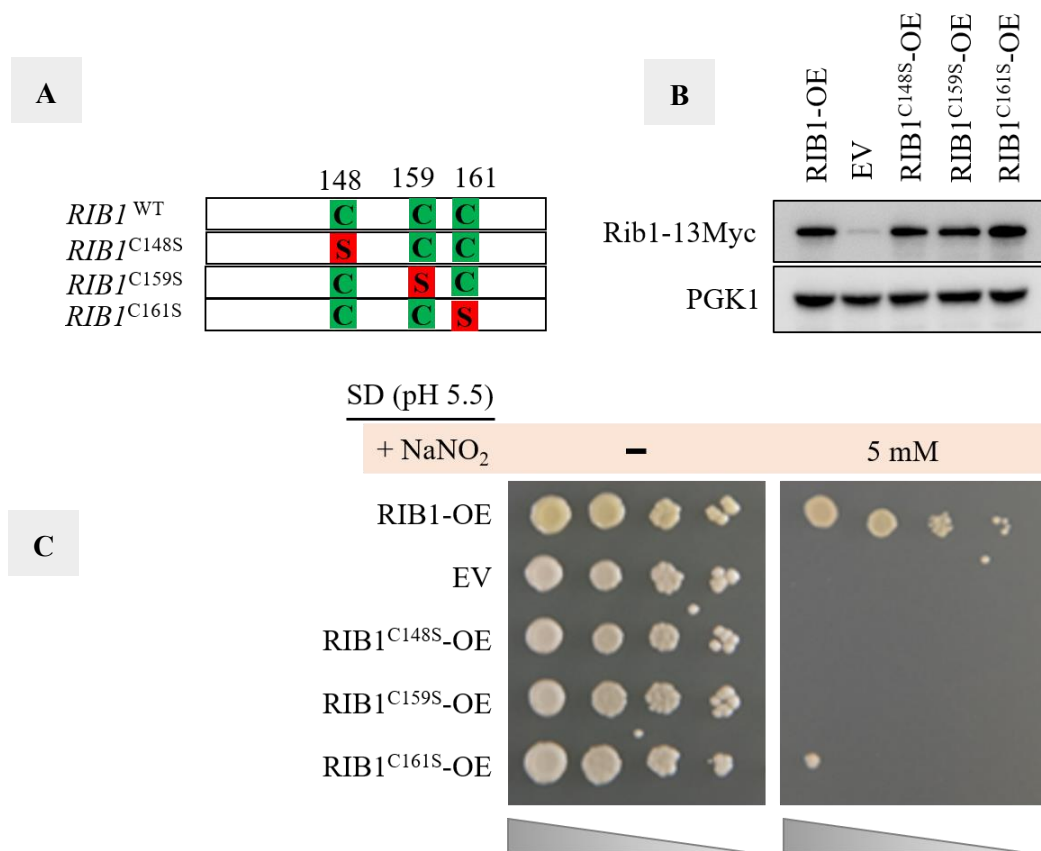
Figure 19. The catalytic activity of Rib1p plays an important role in acidified NO_2^- tolerance.

A. Rib1p-variants: WT, Cys148Ser, Cys159Ser, and Cys161Ser. **B.** Western blot of *S. cerevisiae* BY4741 RIB1-13myc pRS416-CgHIS3-MET15 harboring plasmid pAG415GPD-RIB1-13myc (RIB1-OE), pAG415GPD-ccdB (EV), pAG415GPD-RIB1^{C148S}-13myc (RIB1^{C148S}-OE), pAG415GPD-RIB1^{C159S}-13myc (RIB1^{C159S}-OE), pAG415GPD-RIB1^{C161S}-13myc (RIB1^{C161S}-OE) cells. **C.** Spot test of cells mentioned above on acidified NO_2^- condition. Approximately, $OD_{600} = 1$ cells were 10-fold serially diluted to 10^{-3}, spotted on SD plate at pH 5.5 (control), and SD plate containing 5 mM $NaNO_2$ at pH 5.5, and incubated at 30°C for 2-4 days.

3.8. Overexpression of *RIB1* reduces the intracellular NO level

In Figure 16, RIB1-OE cells showed higher cell viability than controls under excessive NO conditions induced by NOC-5. To investigate whether overexpression of *RIB1* reduces the intracellular NO level, RIB1-OE cells were treated with DAF-FM DA followed by 0.5 mM NOC-5 as an NO donor. The result showed that RIB1-OE cells decreased relative fluorescence intensity compared to controls (Figure 20), suggesting that RIB1-OE cells confer NO tolerance by reducing the intracellular NO level in yeast cells.
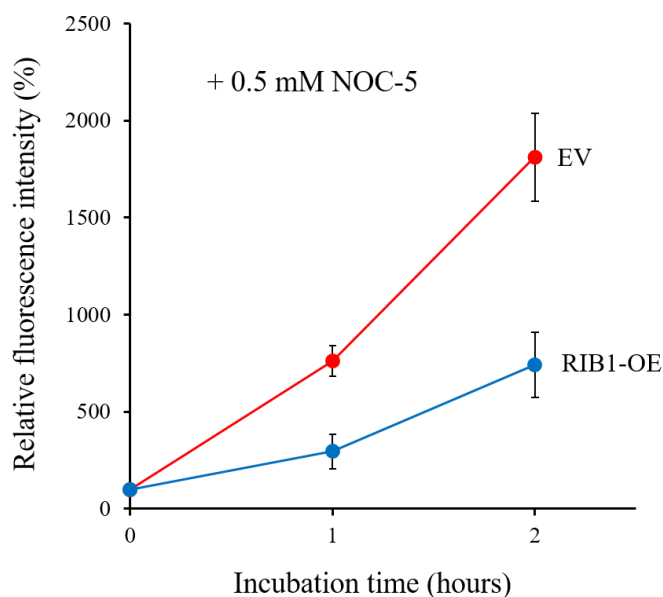
Figure 20. Overexpression of *RIB1* reduces the intracellular NO level in yeast.
Intracellular NO level measurement of *S. cerevisiae* BY4741 RIB1-13myc pRS416-CgHIS3-MET15 harboring plasmid pAG415GPD-RIB1-13myc (RIB1-OE) and pAG415GPD-ccdB (EV) cells. Approximately, $OD_{600} = 1$ cells were dispensed into 1 ml culture volume and 10 μM DAF-FM DA (NO probe) was added 30 minutes before the addition of NOC-5. Afterward, the cells were incubated in SD medium containing 0.5 mM NOC-5 at pH 5.5 for 2 hours at 30°C with 300 rpm agitation. The relative fluorescence intensity was measured by dividing the fluorescence intensity at sampling time with the fluorescence intensity at 0-hour incubation time in percentage. Blue line indicates RIB1-OE cells; red line indicates WT harboring EV. Data are shown in mean ± s.d of three independent experiments.

3.9. Preparation of the purified recombinant Rib1p

The results described above demonstrate that RIB1-OE cells could reduce the intracellular NO level to protect yeast cells from excessive NO. In addition, the catalytic activity of Rib1p contributed to the acidified NO_2^- tolerance of yeast cells. Therefore, it is necessary to clarify whether the catalytic activity of Rib1p is associated with the reduction of intracellular NO level. I hypothesized that Rib1p catalytic activity is associated with reduction of NO through two mechanisms: 1) Rib1p can react with NO directly to detoxify it; or, 2) the reaction product of Rib1p is able to bind or scavenge NO.

To investigate the relationship between the catalytic activity of Rib1p and the reduction of NO level, I prepared recombinant Rib1p (rRib1p) to perform *in vitro* assay. His-tagged rRib1p was purified from *E. coli* transformant cells harboring the *RIB1* gene.

Figure 21 shows Coomassie blue staining of recombinant protein in the crude lysates and purified fraction after Ni-NTA purification. The buffer solution of the purified fraction was changed and then concentrated by Amicon. The molecular weight of rRib1p was around 38 kDa. According to this procedure, rRib1p was purified by affinity column. The enzymatic activity of rRib1p was measured by analyzing the DARP content through derivatization reaction with diacetyl. The DARP content was not directly measured; its derivative, 6,7-dimethylpterin was used to represent the DARP compound, which can be detected by fluorescence spectrophotometer at $\lambda_{Ex} = 330$ nm and $\lambda_{Em} = 435$ nm. From this assay, the specific activity of Rib1p was determined at 3.63 U/mg protein. The purified and concentrated Rib1p were further used for the *in vitro* assay.
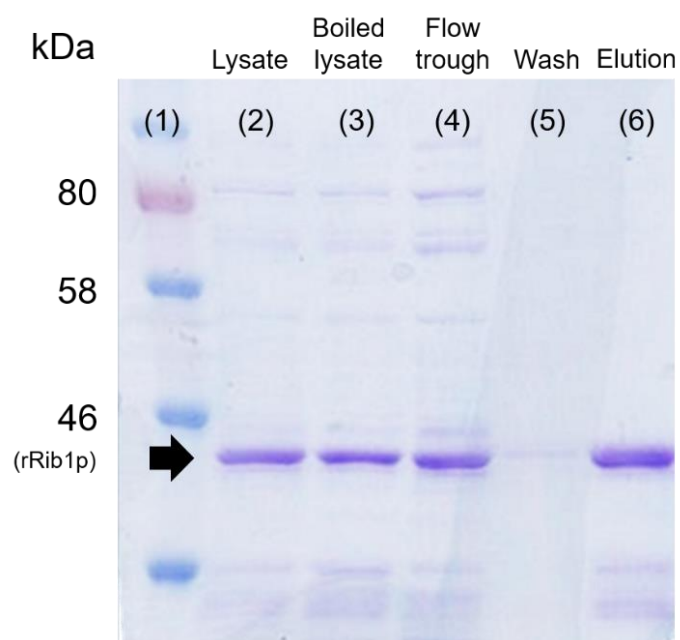

Figure 21. Purification of the recombinant Rib1p.
Lane 1 was a molecular weight marker protein; lane 2 was a *E. coli* lysate; lane 3 was a boiled cell lysate; lane 4 was a flow through buffer solution; lane 5 was an elution buffer solution containing 50 mM imidazole; lane 6 was the elution buffer solution containing 500 mM imidazole.

3.10. Rib1p does not degrade with NO directly

To investigate whether Rib1p directly reacts with NO, Rib1p was mixed with 7 µM DAF-FM, followed by 100 µM NOC-5. In this reaction, NOC-5 released NO and reacted with DAF-FM to form DAF-FM T, a fluorescent benzotriazole that increased the fluorescence intensity representing the NO level. This experiment was performed to confirm whether Rib1p could interfere with the reaction between DAF-FM and NO, and reduce the fluorescence intensity. Results showed that the addition of Rib1p did not reduce fluorescence intensity (Figure 22). The mutant Rib1p and exchanged buffer as blank did not reduce fluorescence intensity either, implying that Rib1p does not directly degrade NO.
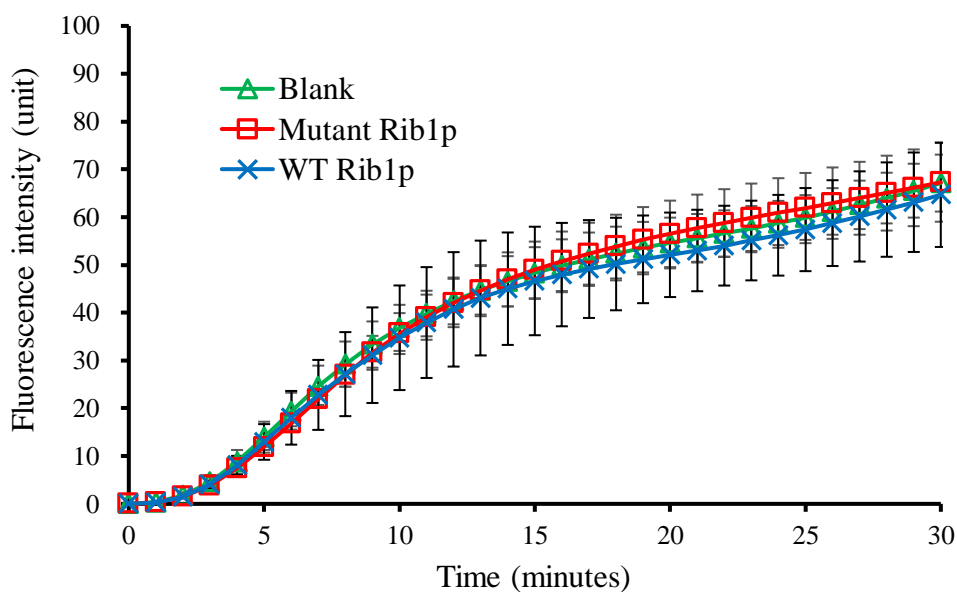

Figure 22. Rib1p is not directly involved in reducing the NO level.
The fluorescence intensity increments of 500 µl solution containing 7 µM DAF-FM, 20 µl sample (exchanged buffer as blank: green triangle; mutant Rib1p (0.60 mg/ml): red square; WT Rib1p (0.66 mg/ml): blue cross), and 100 µM NOC-5 in 100 mM RIB1 assay buffer at pH 7.4 was observed by fluorescence spectrophotometer with $\lambda_{Ex} = 500$ nm and $\lambda_{Em} = 515$ nm for 30 minutes. Data are shown in mean ± s.d of triplicate experiments.

3.11. The reaction product of Rib1p (DARP) quenches NO

Since Rib1p did not reduce the NO level, as a second hypothesis, I investigated whether the Rib1p reaction product, DARP, was responsible for reducing the NO level. However, since DARP as the reaction product of Rib1p is not commercially available, a DARP-containing solution had to be prepared for this experiment. The reaction mixture of Rib1p and GTP as a substrate was incubated for 2 h. Subsequently, the mixed solution was boiled to denature Rib1p, and then spun down to collect the supernatant. The reaction product content, with DARP in the DARP-containing solution, was measured. I then determined whether it could reduce NO level by fluorescence spectrophotometer. In this experiment, the reaction product of a mutant Rib1p, Rib1p without the GTP reaction product, and buffer only were also prepared as controls. As in the previous experiment, the samples were mixed with DAF FM, followed by NOC-5. Results showed that the Rib1p reaction product containing DARP decreased the NO level by lowering fluorescence intensity compared to the controls (Figure 23). This result might be in line with the DARP concentration in each reaction product sample, which in the Rib1p reaction averaged about 25 µM DARP in solution samples; meanwhile, the other reaction products might contain no DARP or less than 1 µM. These results suggest that the Rib1p reaction product containing DARP attenuated the NO level.

The enzymatic activity of Rib1p not only converts GTP into DARP but also produces pyrophosphate (PPi) and formate as byproducts. Therefore, reaction products should contain not only DARP, but also PPi, formate, and unreacted GTP. To find out whether the other compounds contributed to the attenuation of NO level, I made solutions containing them. The NO level was determined by mixing DAF-FM and NOC-5 with these contents alone, except for the DARP-containing solution. In this experiment, the PPi, GTP, and formate solutions concentration was 100 µM. Meanwhile, the DARP concentration in the DARP-containing solution was 25 µM. As shown in Figure 24, only the DARP-containing solution reduced NO level by lowering the fluorescence intensity compared to the other compounds. This indicates that the other compounds did not contribute to the decrease in the NO level.

To examine whether the attenuation of NO level was caused by DARP, different dilution folds of DARP-containing solution were made to determine the concentration

dependency of this phenomenon. As mentioned earlier, the DARP-containing solution also contains other compounds; in these solutions, those compounds were also diluted in the same manner as DARP. Figure 25 shows the solution with smaller dilution fold attenuated the fluorescence intensity more than the solution with higher dilution fold. This suggests that DARP attenuated the NO level in a concentration-dependent manner.
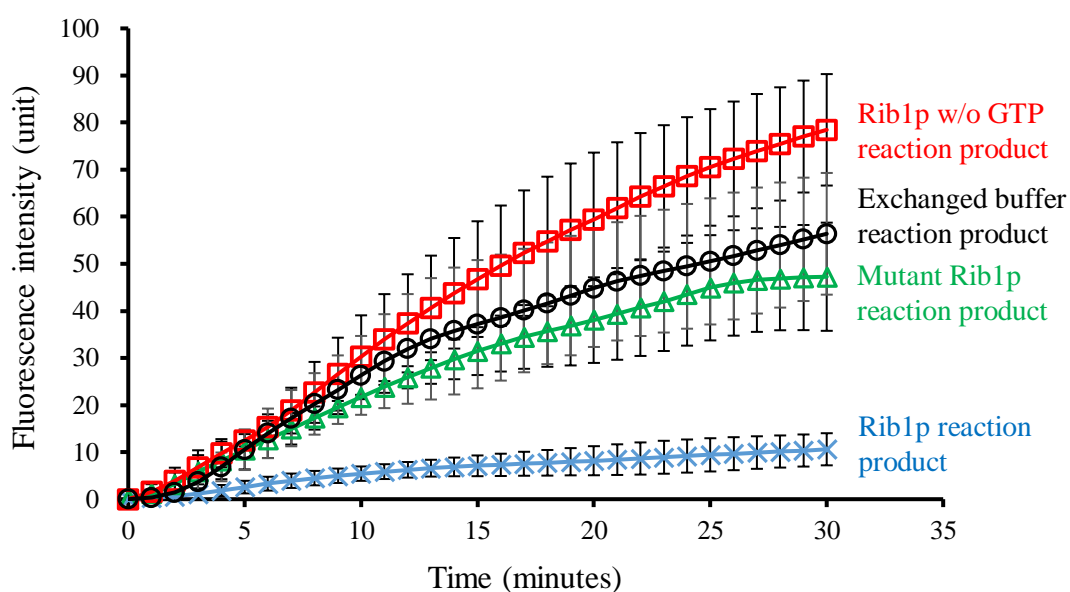

Figure 23. The DARP-containing solution attenuates the NO level.
The fluorescence intensity increments of 500 μl solution containing 7 μM DAF-FM, sample (Rib1p without GTP reaction product = < 1 μM DARP, red square; exchanged buffer reaction product = < 1 μM DARP, black circle; mutant Rib1p reaction product = < 1 μM DARP, green triangle; Rib1p reaction product = < 25 μM DARP, blue cross), and 100 μM NOC-5 in 100 mM RIB1 assay buffer at pH 7.4 was observed by fluorescence spectrophotometer with λ_{Ex} = 500 nm and λ_{Em} = 515 nm for 30 minutes. Data are shown in mean ± s.d of triplicate experiments.
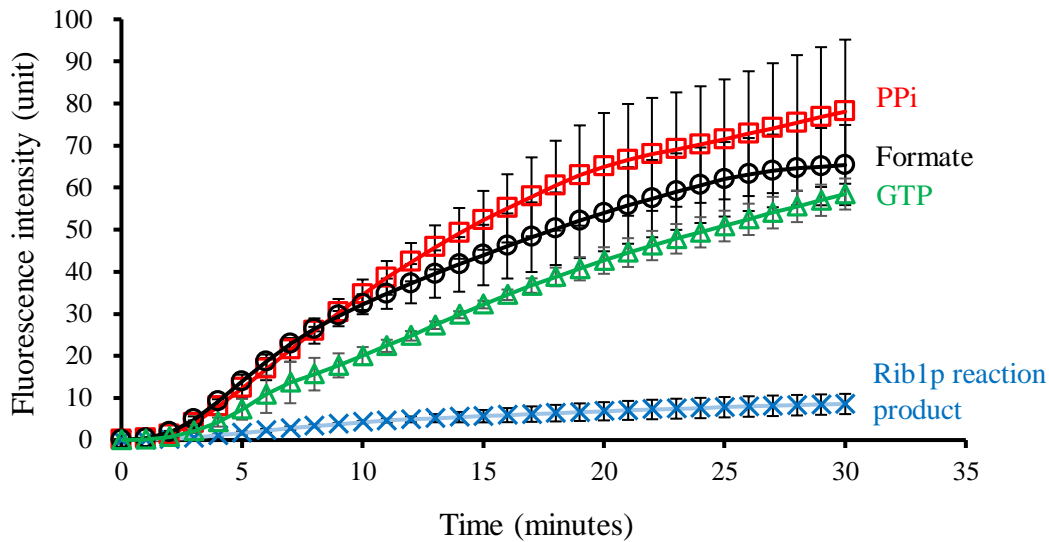
Figure 24. GTP, PPi, and formate do not contribute to the attenuation of the NO level.

The fluorescence intensity increments of 500 μl solution containing 7 μM DAF-FM, sample (100 μM PPi, red square; 100 μM GTP, green triangle; 100 μM formate, black circle; and 25 μM DARP in Rib1p reaction product, blue cross), and 100 μM NOC-5 in 100 mM RIB1 assay buffer at pH 7.4 was observed by fluorescence spectrophotometer with $\lambda_{Ex} = 500$ nm and $\lambda_{Em} = 515$ nm for 30 minutes. Data are shown in mean ± s.d of triplicate experiments.
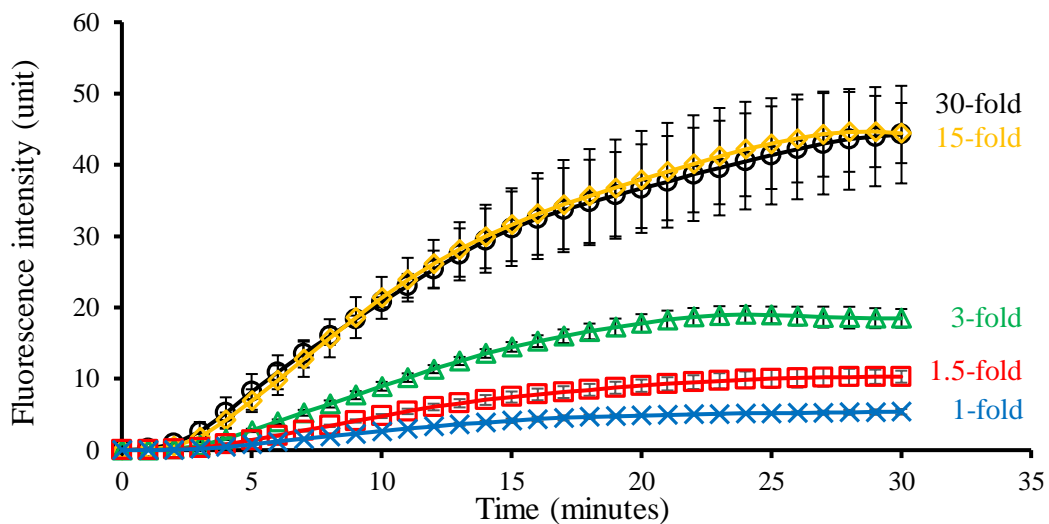

Figure 25. DARP attenuates the NO level in a concentration-dependent manner.

The fluorescence intensity increments of 500 μl solution containing 7 μM DAF-FM, 20 μl sample (DARP-containing solution: 30-fold dilution, black circle; 15-fold dilution, yellow diamond; 3-fold dilution, green triangle; 1.5-fold dilution, red square; 1-fold dilution, blue cross), and 100 μM NOC-5 in 100 mM RIB1 assay buffer at pH 7.4 was observed by fluorescence spectrophotometer with $\lambda_{Ex} = 500$ nm and $\lambda_{Em} = 515$ nm for 30 minutes. Data are shown in mean ± s.d of triplicate experiments.

3.12. Overexpression of *RIB7* does not confer acidified NO$_2^-$ tolerance

In the riboflavin biosynthesis pathway, DARP is a Rib1p product. Subsequently, in this pathway, DARP is converted into DARIP by Rib7p (Figure 5 and Table 2). Given this, overexpression of Rib7p might convert DARP into DARIP more actively, making cells less tolerant under acidified NO$_2^-$ conditions. To investigate the contribution of DARP to acidified NO$_2^-$ tolerance, *RIB7* overexpression cells (RIB7-OE) and *RIB1* plus *RIB7* co-overexpression cells (RIB1-RIB7-OE) were constructed. In Figure 26A, the protein expression from the cells was confirmed by Western blot analysis. Under acidified NO$_2^-$ conditions, both control and RIB7-OE cells showed the same sensitivity (Figure 26B). The same phenotype was also observed in RIB1-OE and RIB1-RIB7-OE cells. This suggests that the overexpression of Rib7p did not reduce acidified NO$_2^-$ tolerance.
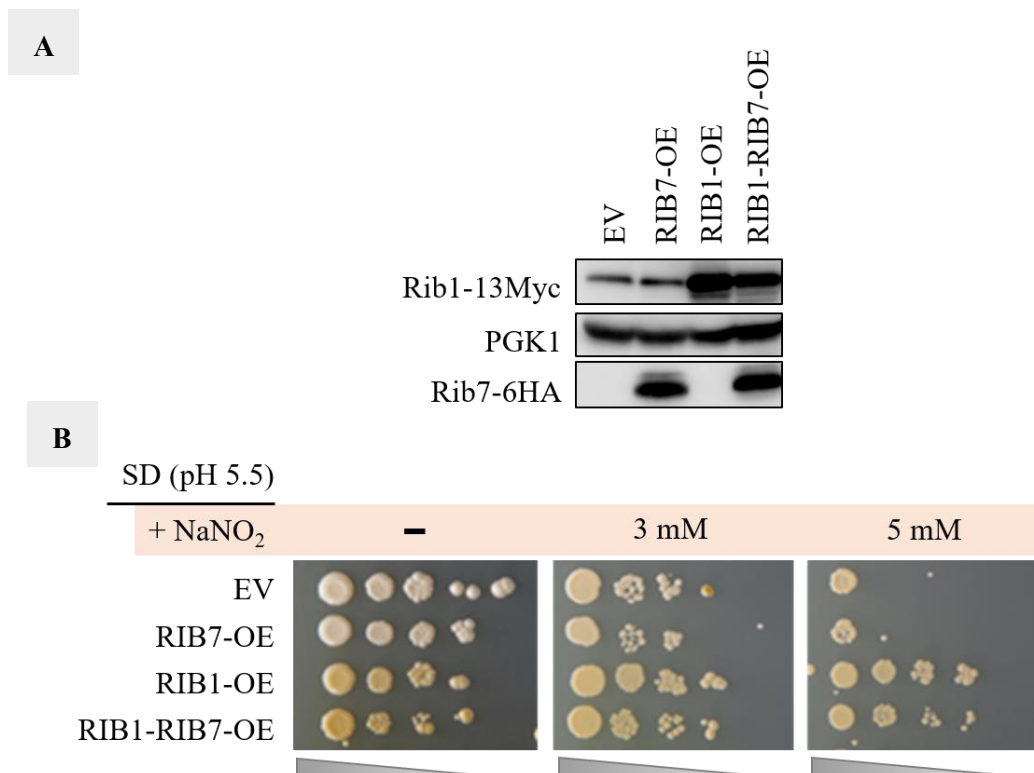

Figure 26. Overexpression of *RIB7* does not confer the acidified NO$_2^-$ tolerance.

A. Western blot of *S. cerevisiae* BY4741 RIB1-13myc pRS416-CgHIS3-MET15 harboring plasmid pAG415GPD-ccdB (EV), pAG415GPD-RIB1-13myc (RIB1-OE), BY4741 RIB1-13myc GPD-RIB7-6HA pRS416-CgHIS3-MET15 harboring plasmid pAG415GPD-ccdB (EV), pAG415GPD-RIB1-13myc (RIB1-OE) cells. **B.** Spot test of cells mentioned above on acidified NO$_2^-$ condition. Approximately, OD$_{600}$ = 1 cells were 10-fold serially diluted to 10^{-3}, spotted on SD plate at pH 5.5 (control), and SD plates containing 3 mM and 5 mM NaNO$_2$ at pH 5.5, and incubated at 30°C for 2-4 days.

3.13. Effects of *RIB* genes disruption on acidified NO_2^- tolerance

For further clarification of whether the conversion of DARP into DARIP is involved in the acidified NO_2^- tolerance, I constructed *RIB* gene-deleted cells harboring RIB1-OE or EV. Deleting the *RIB* genes was expected to elucidate the intermediate molecule involved in the acidified NO_2^- tolerance. In Figure 27A, the expression of Rib1p in cells harboring the RIB1-OE plasmid was confirmed by Western blot analysis. Spot tests showed that overexpression of *RIB1* promoted the acidified NO_2^- tolerance in yeast cells lacking the *RIB* genes, including Δ*rib7* cells, which cannot convert DARP into DARIP due to the lack of *RIB7* that encodes Rib7p (Figure 27B). This finding suggested that DARP, as a reaction product of Rib1p, is the initial compound that promotes the acidified NO_2^- tolerance.

However, in Figure 27C, Δ*rib2* cells showed slightly higher tolerance compared to other *RIB* disruptant cells, including control cells harboring EV. This implies that the accumulation of intermediate product of RF biosynthesis in Δ*rib2* cells has a greater ability to confer stress tolerance than the other cells. This suggests that accumulation of the intermediate product in Δ*rib2* cells, which might accumulate the Rib7p product, DARIP, contribute to the acidified NO_2^- tolerance of yeast cells.
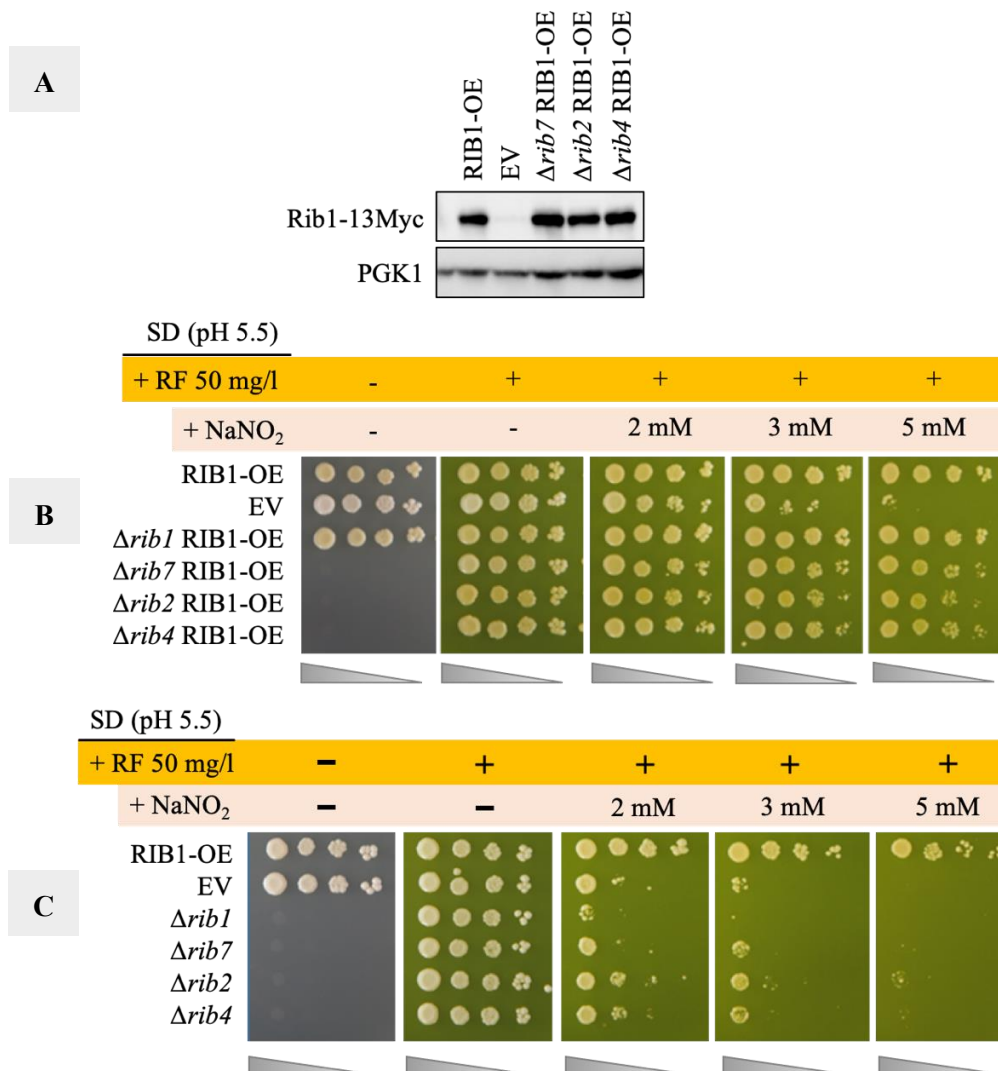
Figure 27. Overexpression of *RIB1* rescues the *RIB* genes-deleted cells under acidified NO₂⁻ conditions.

A. Western blot of *S. cerevisiae* BY4741 RIB1-13myc pRS416-CgHIS3-MET15 harboring plasmid pAG415GPD-RIB1-13myc (RIB1-OE), pAG415GPD-ccdB (EV), BY4741 Δ*rib1*, Δ*rib7*, Δ*rib2*, and Δ*rib4* pRS416-CgHIS3-MET15 harboring plasmid pAG415GPD-RIB1-13myc (RIB1-OE) cells. **B.** Spot test of cells mentioned above on acidified NO₂⁻ condition. Approximately $OD_{600} = 1$ cells were 10-fold serially diluted to 10^{-3}, spotted on SD plate at pH 5.5 (control), and SD plates containing 0, 2, 3, and 5 mM NaNO₂ at pH 5.5 with 50 mg/l riboflavin (RF), and incubated at 30°C for 2-4 days. **C.** Spot test of *S. cerevisiae* BY4741 RIB1-13myc pRS416-CgHIS3-MET15 harboring plasmid pAG415GPD-RIB1-13myc (RIB1-OE), pAG415GPD-ccdB (EV), BY4741 Δ*rib1*, Δ*rib7*, Δ*rib2*, and Δ*rib4* pRS416-CgHIS3-MET15 harboring plasmid pAG415GPD-ccdB (EV) cells on acidified NO₂⁻ condition. Approximately, $OD_{600} = 1$ cells were 10-fold serially diluted to 10^{-3}, spotted on SD plate at pH 5.5 (control), and SD plates containing 0, 2, 3, and 5 mM NaNO₂ at pH 5.5 with 50 mg/l riboflavin (RF), and incubated at 30°C for 2-4 days.

3.14. The triamino-pyrimidine moiety of DARP/DARIP scavenges NO

The results above show that RIB7-OE did not reduce acidified NO_2^- tolerance. These data were supported by the other result that $\Delta rib2$ cells were more tolerant to acidified NO_2^- than control cells, suggesting that DARIP shares the same function for NO tolerance with DARP. I therefore further analyzed the molecule structure of both of DARP and DARIP. As shown in Figures 28A and 28B, DARP and DARIP shared the same moiety in their pyrimidine structure. They also shared the same number of amino groups (three). It should be noted that DARP and DARIP are not currently commercially available. Thus, in order to confirm the involvement of DARP and DARIP in NO tolerance, I found an analogous molecule with a similar structure to DARP and DARIP (Figure 28C). This compound called DARPM (the DARP/DARIP analog) is 2,4,5-triamino-6-hydroxy-pyrimidine. Based on the similar moiety, DARPM was tested in the reaction with NO. As shown in Figure 29, DARPM reduced fluorescence intensity in a concentration-dependent manner, suggesting that DARP and DARIP are both involved in reducing the NO level.
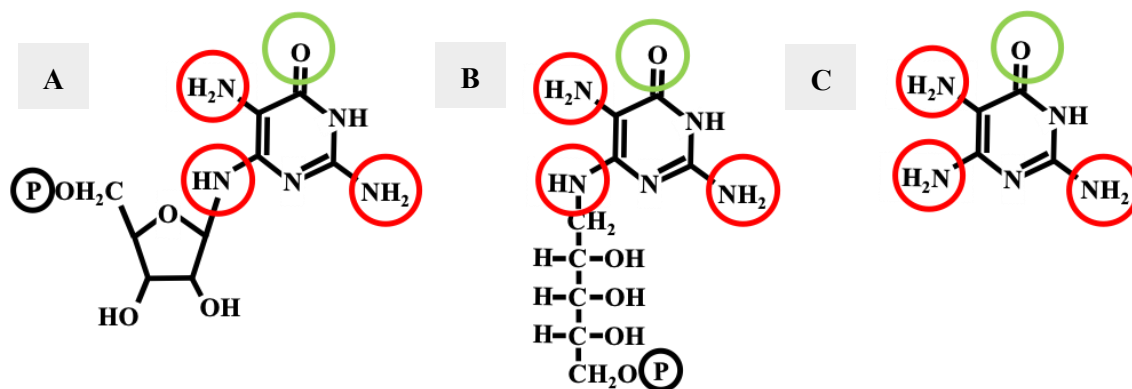

Figure 28. The molecule structure of DARP, DARIP, and DARPM.
A. DARP molecule structure. **B.** DARIP molecule structure. **C.** 2,4,5-Triamino-6-hydroxy-pyrimidine molecule structure (DARP/DARIP moiety analog: DARPM). Red circles indicate amino groups and green circles indicate carbonyl groups.
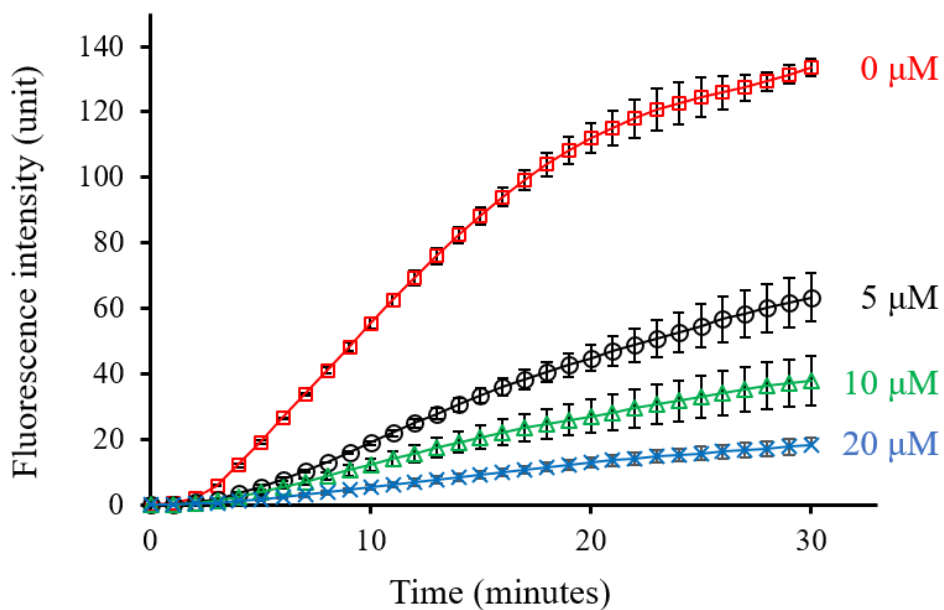
Figure 29. The moiety of DARP and DARIP analog contribute to NO scavenging.

The fluorescence intensity increments of 500 µl solution containing 7-µM DAF-FM, sample (DARPM solution: 0 µM indicates by red square; 5 µM indicates by black circle (n=2); 10 µM indicates by green triangle; 20 µM indicates by blue cross), and 100 µM NOC-5 in 100 mM RIB1 assay buffer at pH 7.4 was observed by fluorescence spectrophotometer with λ_{Ex} = 500 nm and λ_{Em} = 515 nm for 30 minutes. Data are shown in mean ± s.d of triplicate experiments.

3.15. Rib1p expression did not respond to excessive NO level

In this study, I utilized the multicopy plasmid library for screening genes involved in NO tolerance, and found that the plasmid library harboring *RIB1* gene was involved. I subsequently constructed RIB-OE cells for further investigation, and found that the overexpression of *RIB1* confers NO tolerance. However, Δ*rib1* cells were shown to be more sensitive than WT cells harboring EV (Figure 17 and 27). Based on these experiments, I wanted to confirm that the expression of Rib1p under excessive NO level is the expression of *RIB1* that can respond to a higher NO level condition. Therefore, I measured the protein level of Rib1p in the presence of excessive NO induced by an NO donor, NOC-5. The results showed no difference in the protein level of Rib1p in the presence or absence of excessive NO (Figure 30). This result coincided with previous report that the mRNA expression level of *RIB1* was neither upregulated nor downregulated in the presence of excessive NO induced by an NO donor, DETA NONOate (Horan et al. 2006).
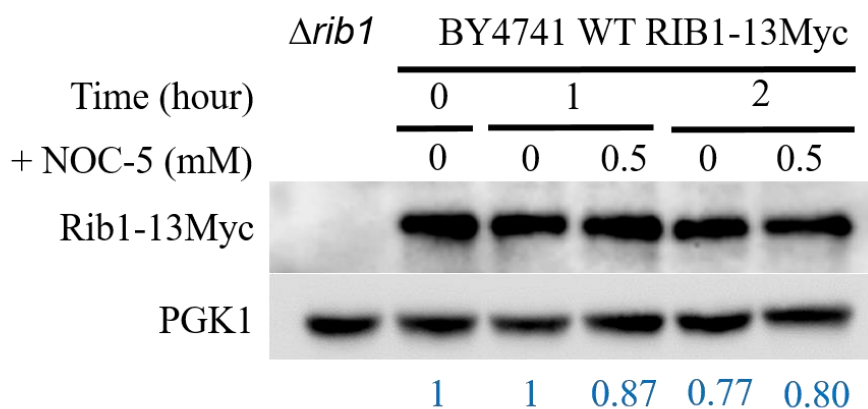

Figure 30. Rib1p expression stays at the same level under excessive NO derived from NO donor, NOC-5.

S. cerevisiae strain BY4741 Δ*rib1* (as negative control) and WT RIB1-13Myc harboring pRS416Cg-HIS3-MET15 and pAG415GPD-ccdB (EV) cells were pre-cultured in 2 ml SD medium at pH 5.5 and then inoculated in 20 ml SD medium at pH 5.5 with initial OD_{600} = 0.05. Cell cultures were incubated at 30°C with agitation at 140 rpm. After reach OD_{600} = 1, cell cultures were dispensed into 2 ml and were treated under excessive NO level in SD medium containing 5 mM NOC-5 and incubated for 2 hours at 30°C with agitation at 300 rpm. Samples were collected every 1 hour for detection of Rib1-13Myc. Number in blue color represents the relative expression of Rib1-13Myc divided by PGK1 and sample at 0 hour was used as a relative comparison.

4. DISCUSSION

The studies on NO tolerance

The cellular functions of NO as a small molecule are dependent on its concentration. At a low or homeostasis level, NO plays a role in physiological processes, whereas at an excessive level, it exerts cytotoxicity on cells. In human cells, a low level of NO promotes tolerance to oxidative stress, vasodilation of smooth muscle, and neurotransmitter release (Benhar et al. 2009). In bacterial cells, a low level of NO also plays a role in the mechanism of oxidative stress tolerance (Allain et al. 2000). In *S. cerevisiae*, our laboratory found that NO confers oxidative stress tolerance through activation of Mac1 on yeast cells (Nasuno et al. 2014). In the absence of a NOS ortholog, our lab found that the flavoprotein Tah18 in *S. cerevisiae* shows NOS-like activity to generate NO from L-arginine (Nishimura et al. 2013). In addition, NO raises cell protection under high-temperature stress in *S. cerevisiae* (Nishimura et al. 2013; Nasuno et al. 2014; Liu et al. 2015). As the pathophysiological effects of excessive NO can cause cellular damage or death, it is important to prevent or detoxify excessive NO to hinder the pathophysiological effects.

Excessive NO level causes severe conditions in cells due to the high reactivity of NO, as RNS, and its derived compounds, such as peroxynitrite. The impact of excessive NO-derived RNS in post-translational modification affects the function of various endogenous proteins, which possess cysteine residues, heme or metal ions, and generate nitrosative stress condition leading to cellular damage or death (Thippeswamy et al. 2006). Therefore, cells must be capable of preventing excessive NO levels to prevent cytotoxic effects.

Several mechanisms have been studied in response to excessive NO levels. The FHb are nitric oxide dioxygenases the expression of which is induced by NO. FHb decreases NO level and promotes NO tolerance by converting NO into nitrate in the presence of oxygen (Forrester et al. 2011). In addition, other oxidoreductase enzymes respond to a higher NO level to detoxify this reactive molecules. Enzymes involved in GSH and Trx systems, both of which show similar functions in yeast and mammalian systems, respond to the stress conditions through transnitrosylation and denitrosylation

processes. GSNOR converts the GSNO into GSSG by releasing ammonia (Benhar et al. 2009). On the other hand, Trx removes NO from the proteins *S*-nitrosothiol (Benhar et al. 2009; Zhou et al. 2013). In yeasts, the well-known mechanisms of NO tolerance are also related to FHb (Tillmann et al. 2011).

In an attempt to find the novel genes required for NO tolerance in *A. nidulans*, Zhou et al. (2012) utilized the multicopy plasmid library under acidified NO_2^- condition and identified porphobilinogen deaminase (PBD-G) as the gene that modulates the reduction of NO level. Other approaches to find novel genes related to NO tolerance include the observation of gene expression, which either up- or downregulated in excessive NO condition compared to the basal condition (Hromatka et al. 2005; Horan et al. 2006; Biswas and Ghosh 2015). In this study, I utilized the multicopy plasmid library to search for the novel genes involved in NO tolerance in *S. cerevisiae* in acidified NO_2^- condition. As an NO source, $NaNO_2$ is capable of releasing NO spontaneously under acidic conditions through protonation and reduction mechanisms (Modin et al. 2001; Shiva 2013). In addition, Stamler et al. (1992) studied the role of $NaNO_2$ in generating NO and *S*-nitrosothiols in the acidified condition (0.5 M HCl). By using ^{15}N-labeled $NaNO_2$ in an *in vitro* chemical analysis, they showed that ^{15}NO is capable of reacting with BSA, which possesses a single free thiol to form *S*-nitroso BSA. In line with those reports, I also observed that intracellular NO level increased in $NaNO_2$ in a concentration-dependent manner at pH 5.5 (Figure 6), which also resulted in the reduction of cell viability (Figure 7). These results suggest a correlation between $NaNO_2$ concentration, intracellular NO level, and cytotoxic effect, as well as the importance of $NaNO_2$ in studying the NO tolerance mechanism.

The involvement of *RIB1* in promoting NO tolerance in *S. cerevisiae*

For the first time, I identified *RIB1* that encodes GTP cyclohydrolase II or Rib1p, as a novel gene implicated in NO tolerance in *S. cerevisia*e. I found that *RIB1* overexpression confers tolerance on *S. cerevisiae* to excessive NO derived from acidified NO_2^- (Figure 14B) and from the NO donor NOC-5 (Figure 16). Moreover, *RIB1* overexpression decreased the intracellular NO level (Figure 20). In contrast, Δ*rib1* cells were more sensitive to acidified NO_2^- than WT cells (Figure 17B), suggesting that *RIB1* is involved in NO tolerance of yeast cells. To further clarify the molecular mechanisms of Rib1p in mediating NO tolerance, I examined the crosslink between Rib1p in the RF biosynthesis pathway with the denitrosylation enzymes in either the Trx or Grx systems, elucidated the involvement of RF and its biosynthesis pathway, and investigated the role of Rib1p catalytic activity, as well as the involvement of the Rib1p main product in NO tolerance in *S. cerevisiae*.

I investigated whether denitrosylation enzymes, which are involved in nitrosative stress tolerance, are associated with the *RIB1*-dependent NO tolerance of *S. cerevisiae*. Rib1p has seven cysteine residues in the molecule that can be targeted by *S*-nitrosylation. Cysteine-rich peptides such as nitrosothionein have been known to scavenge NO, and play a role in nitrosative stress tolerance. This peptide is associated with the Trx system, which is involved in the detoxification of NO derived from acidified NO_2^- by reducing the intracellular *S*-nitrosothiols content (Zhou et al. 2013). Thus, it is possible that Rib1p may also quench NO and interact with denitrosylation enzymes in systems such as the Trx or Grx to neutralize the nitrosylated Rib1p. However, I found that Rib1p was not associated with those systems. The overexpression of Rib1p in cells lacking Trx, Trr, Grx or Glr showed a similar level of cell viability compared to the overexpression of Rib1p in WT cells (Figure 18B). Nevertheless, several mutants lacking a single gene encoding denitrosylation enzymes were shown to be more sensitive than WT cells under the acidified NO_2^- condition, suggesting that those denitrosylation enzymes also play roles in NO detoxification, as reported (Sengupta and Holmgren 2012; Ren et al. 2019). Moreover, these results suggest that the effect of Rib1p under the acidified NO_2^- condition was independent from denitrosylation enzymes such as Trx and Grx.

Yhb1p, a yeast flavohemoglobin (FHb), has been widely reported to play an important role as an NO detoxifying enzyme. Thus, I examined the role of RF as the precursor of FAD, a coenzyme of FHb, and as the final product in the RF biosynthesis pathway promoting NO tolerance. In $\Delta rib1$ cells, RF supplementation in the medium was able to promote cell survival under normal conditions. However, upon exposure to the acidified NO_2^-, RF supplementation was not able to promote NO tolerance or cell protection against acidified NO_2^- condition (Figure 17B). These data suggest that RF is not involved in mediating the Rib1p-dependent NO tolerance mechanism.

As mentioned earlier, Rib1p possesses several cysteine residues (Kaiser et al. 2002). In bacterial GTP cyclohydrolase 2 (GTPCH2), the most well known GTP cyclohydrolases 2 encoded by the *ribA* gene, three cysteine residues at positions Cys54, Cys65 and Cys67 have been reported to bind a Zn ion to initiate the GTP ring opening (Ren et al. 2005). As the first enzyme in the RF biosynthesis, the GTP ring opening via the release of C8, pyrophosphate and formate is ultimately important for GTPCH2 in the formation of DARP (Ren et al. 2005; Gräwert et al. 2013). In addition, the amino acid changes of those cysteine residues diminish the activity of GTPCH2 to produce DARP. As the cysteine residues involved in the Zn^{2+}-binding site are highly conserved among many organisms, including *S. cerevisiae* (Kaiser et al. 2002), the cysteine residues that were changed in this study may affect the Zn^{2+}-binding capacity of the *S. cerevisiae* Rib1p, and contribute to the reduction in NO tolerance. I found that by abolishing the enzymatic activity of Rib1p, the cells overexpressing mutant Rib1p could not survive under excessive NO level derived from acidified NO_2^-, suggesting that the catalytic activity of Rib1p plays an important role in the NO tolerance mechanism (Figure 19C). As the catalytic activity of Rib1p is important for hydrolyzing the imidazole ring of the GTP molecule, without this catalytic activity, DARP might not be produced (Kaiser et al. 2002). This suggests that DARP, as a main Rib1p product, might be involved in the Rib1p-dependent NO tolerance mechanism. DARP possesses the ortho-diamino group in its moiety which may play a role in quenching NO and alleviating the excessive NO condition in *S. cerevisiae* (Figures 23, 24, and 25).

A possible mechanism for NO quenching by DARP, its derivatives, and the diamino group compounds

Rib1p catalyzes the conversion of GTP into DARP. I observed that Rib1p in an *in vitro* enzymatic reaction mixture containing DARP, interfered with the reaction between DAF FM and NO, suggesting that DARP acts as an NO scavenger (Figure 23, 24, and 25). To clarify that DARP plays a role in NO tolerance, I sought to determine intracellular DARP levels in WT cells harboring the EV, and RIB1-OE, and in Δ*rib1*. However, as these three strains showed different growth phenotypes in the presence of excessive NO induced by acidified NO_2^- (Figure 17B), I hypothesized that intracellular DARP content was different among them, affected by Rib1p expression level. On the other hand, the derivative molecules of DARP (i.e., DARIP and ARIP), may also react with NO. DARIP is the Rib7p reaction product with DARP as the substrate. The role of DARIP in NO tolerance was suggested by the overexpression of *RIB7*, which might be reduced NO tolerance in yeast cells. However, the different phenotypes were not observed in RIB1-OE in comparison to RIB1-RIB7-OE cells or in RIB7-OE in comparison to WT cells harboring the EV under acidified NO_2^- condition (Figure 26B). Meanwhile, ARIP is the Rib2p reaction product with DARIP as the substrate. As shown in Figure 27C, the *RIB2*-deleted cells (Δ*rib2*) showed higher NO tolerance compared to WT cells, suggesting that Rib7p product DARIP might be accumulated in Δ*rib2* cells to enhance the NO tolerance in an acidified NO_2^- condition. Overall, these results showed that DARIP also contributes to NO tolerance. Since DARP and DARIP have the same moiety in their pyrimidine structure, the reaction of DARP or DARIP with diacetyl forms the same product, 6,7-dimethylpterin (Figure 28). This result can be confirmed by using DARPM as the DARP/DARIP moiety analog.

Screening the genes with the plasmid library revealed that every gene had the similar probability to be overexpressed. However, from the screening process, only *RIB1* was identified as a candidate, not *RIB7* that was related to formation of DARIP from DARP. I hypothesize that when *RIB1* was overexpressed, Rib1p will convert GTP into DARP, in which the availability of GTP is abundant. However, in RIB7-OE cells, the availability of DARP as the substrate of Rib7p is low, thus limiting the production and accumulation of DARIP to confer NO tolerance. Therefore, Rib1p, as the first enzyme

involved in RF biosynthesis, plays a key role in providing DARP as the substrate of the downstream enzymes in the pathway to quench NO.

DARP and DARIP share the same position as the three amino groups in the pyrimidine structure (Figure 28) that may act as NO scavenger, as confirmed by their moiety analog, DARPM (Figure 29). I further analyzed the similarity between the DARP structure and an NO probe and found that the reaction mechanism between DARP and NO might be similar to the reaction between DAF-FM and NO. As shown in Figure 31A, the reaction between DAF-FM and NO forms the DAF-FM triazole, (Namin et al. 2013; Kępczyński and Lech 2018) whereas the reaction between 2,3-diaminonaphthalene and nitrosyl (NO_x) also forms a triazole formation (1H-naphtha triazole) (Figure 31B) (Bryan and Grisham 2007; Hu et al. 2014). DAF-FM and DAN share a similar diamino group moiety at the ortho position, which might be the key to the NO scavenging reaction. Therefore, I predicted a hypothetical reaction between DARP and NO involving triazole formation (Figure 31C). Although DARP has a similar moiety with DAF-FM and DAN, further study is needed to clarify this hypothetical reaction between DARP and NO. Moreover, since DARIP and ARIP also possess the same moiety as DARP (Figure 32), a similar hypothetical reaction may also occur for DARP derivatives.

To clarify the reaction between DARP and NO, a pure form of DARP is needed. However, DARP is not currently commercially available, and so chemical syntheses of these compounds is required. Production of DARP can be performed through the *in vitro* enzymatic reactions or *in vivo* metabolic engineering. The purified molecule must be confirmed by structural elucidation, including mass spectra (MS), carbon nuclear magnetic resonance (C-NMR), proton nuclear magnetic resonance (H-NMR) and infrared (IR) spectroscopy. After the structural determination, these molecules could be used for the chemical reaction with NO. Using DARPM instead of DARP would also suffice to determine the reaction product with NO. Moreover, the molecular structure of the products, which may contain triazole, also needs to be elucidated. Further studies on the reaction between DARP, DARIP and ARIP with NO are needed to clarify the role of Rib1p in NO tolerance in *S. cerevisiae* via DARP and its derivatives.

The implication of Rib1p in NO tolerance mechanism

Excessive NO level is implicated in the generation of neurodegenerative diseases, as well as cell protection from pathogens. In neurodegenerative diseases, excessive NO level is caused by the overproduction of NO by i-NOS (Yuste et al. 2015; Nakato et al. 2015). Since DARP, DARIP, and ARIP can react with NO, they might be potential candidates for reducing excessive levels of NO in neuronal cells for the treatment of neurodegenerative diseases. In addition to their potential as neurodegenerative drugs, DARP, DARIP, and ARIP can be utilized as new NO probes based on their ability to react with NO. On the other hand, Δ*rib2* cells showed slightly higher tolerance compared to other *RIB* disruptant cells, including Δ*rib7* and Δ*rib4* cells (Figure 27C). This suggests that the accumulated reaction products, whether DARP, DARIP or ARIP, possess different reactivity to NO, depending on their chemical structure. In Δ*rib2* cells, DARIP might be accumulated as a Rib7p product; in Δ*rib7* cells, DARP might be accumulated; whereas, in Δ*rib4* cells, it may be that ARIP accumulates. As shown in Figure 27C, DARIP might have higher activity compared to the other products. DARIP might share the same moiety with DARP, but not have a ribosyl group because of the reductase activity of Rib7p. Meanwhile, DARIP and ARIP have a different number of amino groups in their pyrimidine structures. DARIP has three amino groups, while ARIP has only two (Figure 32). In ARIP, the other amino group is converted into carbonyl group by the deaminase activity of Rib2p. This hypothesis might be beneficial for developing new probes or drugs with higher activity to scavenge NO.

On the other hand, the excessive NO level generated by i-NOS also plays an antimicrobial role to overcome infection of the human body from the pathogenic yeasts *C. albicans*. *C. albicans* enters the human body and causes candidiasis. However, as it was observed that depletion of Rib1p increases the susceptibility of yeast cells to excessive NO, development of inhibitors for the *RIB1* gene or Rib1p could be promising antimicrobial drugs. These inhibitors have a synergetic activity with NO to eradicate the pathogens if Rib1p of *C. albicans* has the same effect as in *S. cerevisiae*.
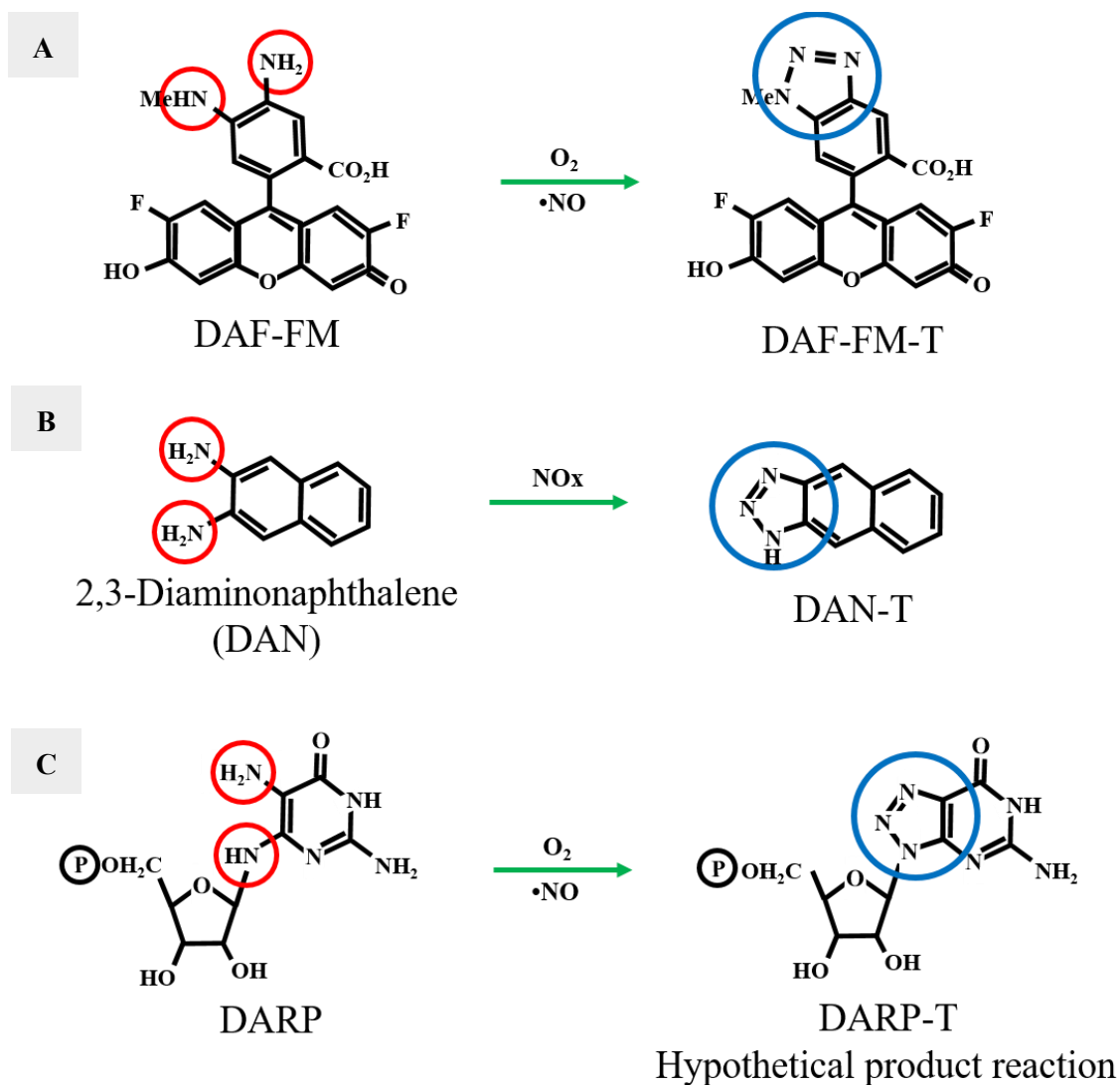
Figure 31. Chemical reactions of DAF-FM, DAN, and DARP with NO, which are involved in triazole formation.

A. DAF-FM reaction with NO form DAF-FM triazole. **B.** 2,3-Diaminonaphthalene (DAN) reaction with nitrosyl (NO_x) form DAN triazole **C.** Proposed reaction between DARP and NO, which form a hypothetical reaction product of DARP with triazole moiety. Red circles indicate the ortho-diamino groups; blue circles indicate triazole structures.
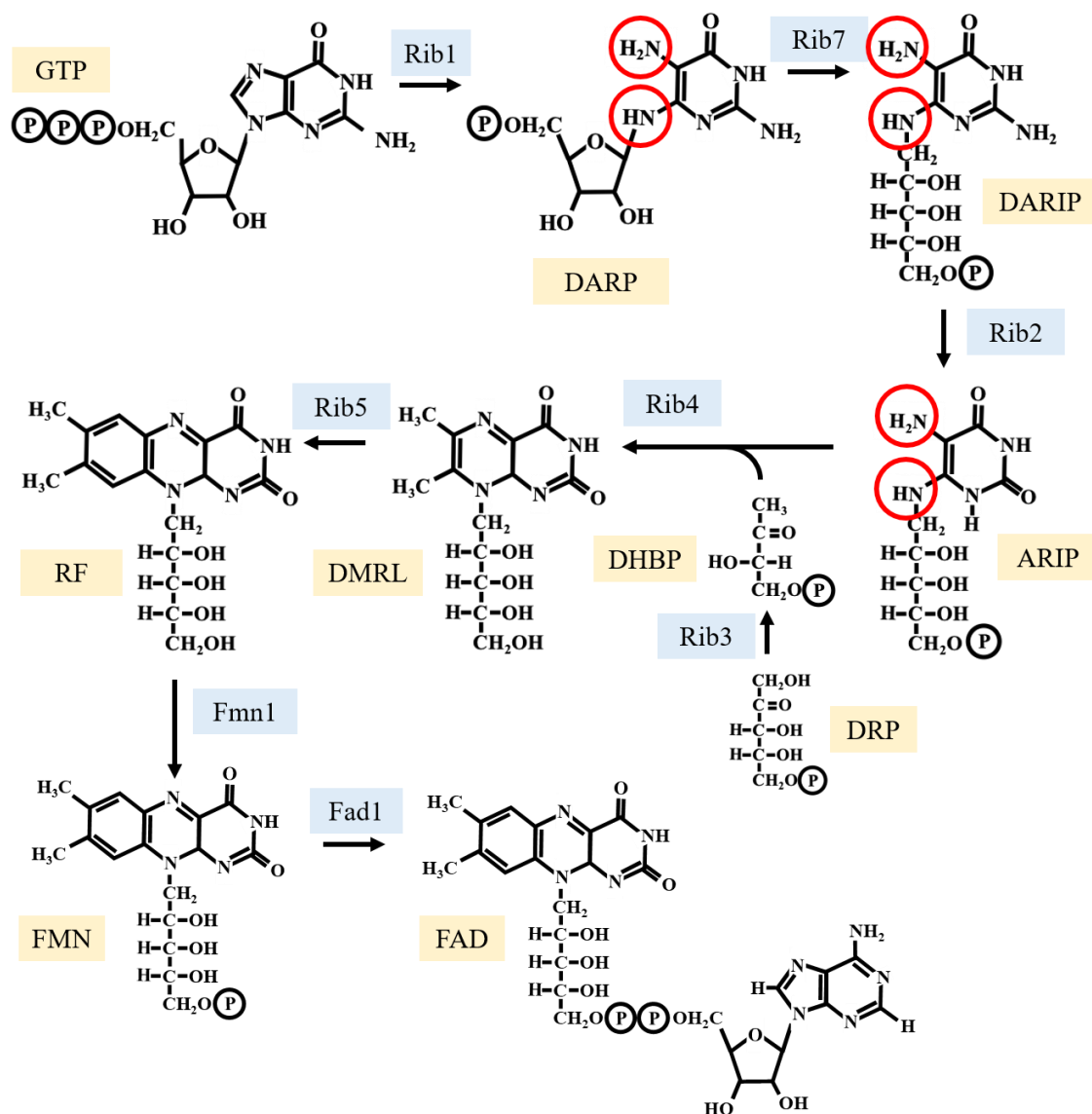
Figure 32. The riboflavin biosynthesis pathway in *S. cerevisiae*.

DARP and its derivatives, DARIP and ARIP, are intermediate molecules, which involved in the riboflavin biosynthesis pathway; share the same moiety of diamino groups at the ortho position (indicated by red circles).

The proposed mechanism of the *RIB1*-dependent NO tolerance in *S. cerevisiae* is shown in Figure 33. The novel finding of this study is that the *RIB1* gene is involved in NO tolerance. Excessive NO levels induce accumulation of RNS (NO and its derivatives), leading to cell damage or death. This condition was inhibited by the overexpression of Rib1p, which converts GTP into DARP. DARP could scavenge NO by forming DARP-triazole, which then reduces NO level. The reduction of NO level cancels the accumulation of RNS, prevents a pathophysiological condition in cells, and averts cell death.
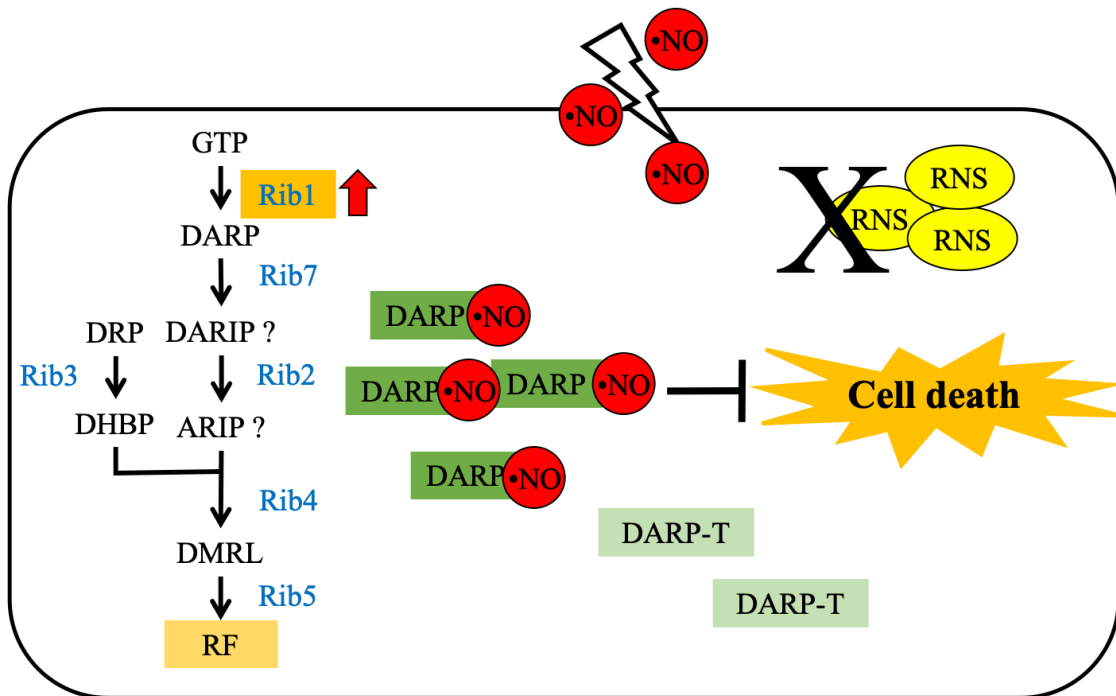
Figure 33. Proposed mechanism of Rib1p-dependent NO tolerance in *S. cerevisiae*.

5. CONCLUSIONS

Excessive NO level has been widely implicated in pathophysiological conditions in both prokaryotic and eukaryotic cells. In the present study, I proposed a new mechanism for NO tolerance based on the plasmid library screening in the yeast *S. cerevisiae*, a well-established model for higher eukaryotes. *RIB1* was identified as a novel gene that plays a role in generating the NO tolerance mechanism in *S. cerevisiae*. The *RIB1* gene encodes Rib1p, an important enzyme in the first step of riboflavin biosynthesis to catalyze the conversion of GTP into DARP. Interestingly, the role of Rib1p in NO tolerance is not associated with the function of the denitrosylation enzymes to detoxify NO, but rather is correlated with its role in riboflavin biosynthesis, including its catalytic activity and main reaction product, DARP. Meanwhile, riboflavin itself is not involved in provoking NO tolerance in *S. cerevisiae*. The DARP ability to quench NO results in the attenuation of the intracellular NO level, which contributes to NO tolerance. Moreover, it was suggested that DARP derivatives, DARIP and ARIP, which possess ortho-diamino groups in their pyrimidine rings, are also involved in quenching excessive NO levels. Nevertheless, further studies to elucidate the reactions of DARP, DARIP, or ARIP with NO are necessary to clarify the role of Rib1p-dependent NO tolerance in *S. cerevisiae* via DARP and its derivatives.

6. ACKNOWLEDGEMENTS

Ikoma, July 29, 2019

Khairul Anam

7. REFERENCES

Abbas, Charles A, and Andriy A Sibirny. 2011. "Genetic Control of Biosynthesis and Transport of Riboflavin and Flavin Nucleotides and Construction of Robust Biotechnological Producers." *Microbiology and Molecular Biology Reviews* 75 (2): 321-60.

Akada, R, J Yamamoto, and I Yamashita. 1997. "Screening and Identification of Yeast Sequences that Cause Growth Inhibition when Overexpressed." *Molecular and General Genetics* 254: 267–74.

Allain, Alexander V, Van T Hoang, George F Lasker, Edward A Pankey, N Subramanyam, and Philip J Kadowitz. 2011. "Role of Nitric Oxide in Developmental Biology in Plants, Bacteria, and Man." *Current Topics in Pharmacology* 15 (2): 25–33.

Almeida, B, S Buttner, S Ohlmeier, A Silva, A Mesquita, Belém S Marques, Nunu S Osório, A Kollau, B Mayer, C Leão, J Laranjinha, F Rodrigues, F Madeo, and P Ludovico. 2007. "NO-Mediated Apoptosis in Yeast." *Journal of Cell Science*, 120 (18): 3279–88.

Bacher, A, S Eberhardt, M Fischer, K Kis, and G Richter. 2000. "Biosynthesis of Vitamin B$_2$ (Riboflavin)." *Annual Review of Nutrition* 20:153-67.

Benhar, M. 2015. "Nitric Oxide and the Thioredoxin System: A Complex Interplay in Redox Regulation." *Biochimica et Biophysica Acta* 1850: 2476–84.

Benhar, M, Michael T Forrester, and Jonathan S Stamler. 2009. "Protein Denitrosylation: Enzymatic Mechanisms and Cellular Functions." *Nature Reviews Molecular Cell Biology* 10 (10): 721–32.

Biswas, P and S Ghosh. 2015. "Global Transcriptomic Profiling of *Schizosaccharomyces pombe* in Response to Nitrosative Stress." *Gene* 558 (2): 241–53.

Broach, James R. Yu Y Li, Ling-Chuan C Wu, and M Jayaram. 1983. "Vectors for High-Level, Inducible Expression of Cloned Genes in Yeast". Experimental Manipulation of Gene Expression, M Inouye, ed. (New York: Academic Press), pp. 83-117.

Brown, Guy C. 2001. "Regulation of Mitochondrial Respiration by Nitric Oxide Inhibition of Cytochrome c Oxidase." *Biochimica et Biophysica Acta - Bioenergetics* 1504 (1): 46–57.

Bryan, Nathan S, and Matthew B Grisham. 2007. "Methods to Detect Nitric Oxide and Its Metabolites in Biological Samples." *Free Radical Biology and Medicine*, 43 (5): 645-57.

Chiranand, W, I McLeod, H Zhou, Jed J Lynn, Luis A Vega, H Myers, John R Yates, Michael C Lorenz, and Michael C Gustin. 2008. " CTA4 Transcription Factor Mediates Induction of Nitrosative Stress Response in *Candida albicans*." *Eukaryotic Cell* 7 (2): 268–78.

Considine, Michael J, Luisa M Sandalio, and Christine H Foyer. 2015. "Unravelling How Plants Benefit from ROS and NO Reactions, While Resisting Oxidative Stress," *Annals of Botany* 116: 469–73.

Cooper, Chris E. 1999. "Nitric Oxide and Iron Proteins." *Biochimica et Biophysica Acta - Bioenergetics* 1411 (2–3): 290–309.

Denninger, John W, and Michael A Marletta. 1999. "Guanylate Cyclase and the NO/cGMP Signaling Pathway." *Biochimica et Biophysica Acta* 1411 (2–3): 334–50.

Feng, X, T Sun, Y Bei, S Ding, W Zheng, Y Lu, and P Shen. 2013. "*S*-Nitrosylation of ERK Inhibits ERK Phosphorylation and Induces Apoptosis." *Scientific Reports* 3:1814.

Ferrer-sueta, G, and R Radi. 2009. "Chemical Biology of Peroxynitrite : Kinetics, Diffusion, and Radicals" *ACS Chemical Biology* 4 (3): 161–77.

Forrester, Michael T, Christine E Eyler, and Jeremy N Rich. 2011. "Bacterial Flavohemoglobin: A Molecular Tool to Probe Mammalian Nitric Oxide Biology." *Biotechniques* 50 (1): 41–45.

Förstermann, U, and William C Sessa. 2012. "Nitric Oxide Synthases: Regulation and Function." *European Heart Journal* 33 (7): 829–37.

Gardner, Paul R, Anne M. Gardner, Lori A Martin, and Andrew L Salzman. 1998. "Nitric Oxide Dioxygenase: An Enzymic Function for Flavohemoglobin" *Proceedings of the National Academy of Sciences of the United States of America* 95 (9): 10378–83.

Gardner, Paul R, Anne M Gardner, Lori A Martin, Y Dou, T Li, John S Olson, H Zhu, and Austen F Riggs. 2000. "Nitric-Oxide Dioxygenase Activity and Function of Flavohemoglobins." *Journal of Biological Chemistry* 275 (41): 31581–87.

Gelaude, A, M Marin, K Cailliau, M Jesetta, Rousseau A Lescuver, P Vandame, J Nevoral, M Sedmikova, A Martoriati, and J F Bodart. 2015. "Nitric Oxide Donor *S*-Nitroso-*N*-Acetyl Penicillamine (SNAP) Alters Meiotic Spindle Morphogenesis in *Xenopus Oocytes*." *Journal of Cellular Biochemistry* 116 (11): 2445-54.

Gräwert, T, M Fischer, and A Bacher. 2013. "Structures and Reaction Mechanisms of GTP Cyclohydrolases." *IUBMB Life* 65 (4): 310–22.

Grossi, L and S D'Angelo. 2005. "Sodium Nitroprusside: Mechanism of NO Release Mediated by Sulfhydryl-Containing Molecules." *Journal of Medicinal Chemistry* 48 (7): 2622-6.

Gu, Z, T Nakamura, and S A Lipton. 2010. "Redox Reactions Induced by Nitrosative Stress Mediate Protein Misfolding and Mitochondrial Dysfunction in Neurodegenerative Diseases." *Molecular Neurobiology* 41 (0): 55–72.

Gudipati, V, K Koch, Wolf D Lienhart, and P Macheroux. 2014. "The Flavoproteome of the Yeast *Saccharomyces cerevisiae*." *Biochimica et Biophysica Acta - Proteins and Proteomics* 1844 (3): 535–44.

Hess, Douglas T, A Matsumoto, Sung O Kim, Harvey E Marshall, and Jonathan S Stamler. 2005. "Protein *S*-Nitrosylation: Purview and Parameters." *Nature Reviews Molecular Cell Biology* 6 (2): 150–66.

Hess, Douglas T, and Jonathan S Stamler. 2012. "Regulation by *S*-Nitrosylation of Protein Post-Translational Modification." *Journal of Biological Chemistry* 287 (7): 4411–18.

Horan, S, I Bourges, and B Meunier. 2006. "Transcriptional Response to Nitrosative

Stress in *Saccharomyces cerevisiae*." *Yeast* 23 (7): 519–35.

Hromatka, Bethann S, Suzanne M Noble, and Alexander D Johnson. 2005. "Transcriptional Response of *Candida albicans* to Nitric Oxide and the Role of the *YHB1* Gene in Nitrosative Stress and Virulence[D]." *Molecular Biology of the Cell* 16 (10): 4814–26.

Hu, The M, Shih J Chiu, and Yu M Hsu. 2014. "Nitroxidative Chemistry Interferes with Fluorescent Probe Chemistry: Implications for Nitric Oxide Detection Using 2,3-Diaminonaphthalene." *Biochemical and Biophysical Research Communications* 451 (2): 196-201.

Janke, C, et al. 2004. "A Versatile Toolbox for PCR-Based Tagging of Yeast Genes: New Fluorescent Proteins, More Markers and Promoter Substitution Cassettes." *Yeast* 21 (11): 947–62.

Kaiser, J, N Schramek, S Eberhardt, S Püttmer, M Schuster, and A Bacher. 2002. "Biosynthesis of Vitamin B_2. An Essential Zinc Ion at the Catalytic Site of GTP Cyclohydrolase II." *European Journal of Biochemistry* 269 (21): 5264–70.

Kępczyński, J and Danuta C Lech. 2018. "Application of Flow Cytometry with a Fluorescent Dye to Measurement of Intracellular Nitric Oxide in Plant Cells." *Planta* 248 (2): 279-91.

Knop, M, K Siegers, G Pereira, W Zachariae, B Winsor, K Nasmyth, and E Schiebel. 1999. "Epitope Tagging of Yeast Genes Using a PCR-Based Strategy: More Tags and Improved Practical Routines." *Yeast* 15: 963–72.

Lima, B, Michael T Forrester, Douglas T Hess, and Jonathan S Stamler. 2010. "*S*-Nitrosylation in Cardiovascular Signaling." *Circulation Research* 106 (4): 633–46.

Liu, L, M Zeng, A Hausladen, J Heitman, and Jonathan S Stamler. 2000. "Protection from Nitrosative Stress by Yeast Flavohemoglobin." *Proceedings of the National Academy of Sciences of the United States of America* 97 (9): 4672–76.

Liu, W Cheng, Hong M Yuan, Yun H Li, and Ying T Lu. 2015. "CKA2 Functions in H_2O_2-Induced Apoptosis and High-Temperature Stress Tolerance by Regulating NO Accumulation in Yeast." *FEMS Yeast Research* 15 (6): fov051.

Lu, N, C Chen, Y He, R Tian, Q Xiao, and Y Peng. 2014. "Nitric Oxide The Dual Effects of Nitrite on Hemoglobin-Dependent Redox Reactions." *Nitric Oxide* 40: 1–9.

Majumdar, U, P Biswas, Tuhin S Sarkar, D Maiti, and S Ghosh. 2012. "Regulation of Cell Cycle and Stress Responses under Nitrosative Stress in *Schizosaccharomyces pombe*." *Free Radical Biology and Medicine* 52 (11–12): 2186–2200.

Matsuo, Y, K Asakawa, T Toda, and S Katayama. 2006. "A Rapid Method for Protein Extraction from Fission Yeast." *Bioscience, Biotechnology, and Biochemistry* 70 (8): 1992–94.

Modin, A, H Björne, M Herulf, K Alving, E Weitzberg, and J O N Lundberg. 2001. "Nitrite-Derived Nitric Oxide: A Possible Mediator of 'Acidic-Metabolic' Vasodilation." *Acta Physiologica Scandinavica* 171 (1): 9–16.

Nakato, R, Y Ohkubo, A Konishi, M Shibata, Y Kaneko, T Iwawaki, T Nakamura, Stuart A. Lipton, and T Uehara. 2015. "Regulation of the Unfolded Protein Response

via *S*-Nitrosylation of Sensors of Endoplasmic Reticulum Stress." *Scientific Reports* 5 (9): 1–9.

Namin, Shabnam M, S Nofallah, Mahesh S Joshi, K Kavallieratos, and Nikolaos M Tsoukias. 2013. "Kinetic analysis of DAF-FM Activation by NO: Toward Calibration of an NO-Sensitive Fluorescent Dye." *Nitric Oxide* 28:39-46.

Nasuno, R, M Aitoku, Y Manago, A Nishimura, Y Sasano, and H Takagi. 2014. "Nitric Oxide-Mediated Antioxidative Mechanism in Yeast Through the Activation of the Transcription Factor Mac1." *PLoS ONE* 9 (11): 1–18.

Nathan, C, and Michael U Shiloh. 2000. "Reactive Oxygen and Nitrogen Intermediates in the Relationship between Mammalian Hosts and Microbial Pathogens" *Proceedings of the National Academy of Sciences of the United States of America* 97 (16): 8841–48.

Nishida, I, D Watanabe, A Tsolomonbaatar, T Kaino, I Ohtsu, and H Takagi. 2016. "Vacuolar Amino Acid Transporters Upregulated by Exogenous Proline and Involved in Cellular Localization of Proline in *Saccharomyces cerevisiae***." *The Journal of General and Applied Microbiology* 62 (3): 132-9.

Nishimura, A, N Kawahara, and H Takagi. 2013. "The Flavoprotein Tah18-Dependent NO Synthesis Confers High-Temperature Stress Tolerance on Yeast Cells." *Biochemical and Biophysical Research Communications* 430 (1): 137–43.

Poole, R K. 2005. "Nitric Oxide and Nitrosative Stress Tolerance in Bacteria', Biochemical Society Transactions 33 (1): 176-80

Powers, Hilary J. 2003. "Riboflavin (Vitamin B-2) and Health". *The American Journal of Clinical Nutrition* 77 (6): 1352–60.

Reihl, P, and J Stolz. 2005. "The Monocarboxylate Transporter Homolog Mch5p Catalyzes Riboflavin (Vitamin B_2) Uptake in *Saccharomyces cerevisiae*." *Journal of Biological Chemistry* 280 (48): 39809-17.

Ren, J, M Kotaka, M Lockyer, H K Lamb, A R Hawkins, and D K Stammers. 2005. "GTP Cyclohydrolase II Structure and Mechanism." *The Journal of Biological Chemistry* 280 (44): 36912–19.

Ren, X, R Sengupta, J Lu, Jon O Lundberg, and A Holmgren. 2019. "Characterization of Mammalian Glutaredoxin Isoforms as *S*-Denitrosylases." *Federation of European Biochemical Societies letters* 593: 1799-1806.

Ridnour, Lisa A, Douglas D Thomas, D Mancardi, Michael G Espey, Katrina M Miranda, N Paolocci, M Feelisch, J Fukuto, and David A Wink. 2004. "The Chemistry of Nitrosative Stress Induced by Nitric Oxide and Reactive Nitrogen Oxide Species. Putting Perspective on Stressful Biological Situations." *Biological Chemistry* 385 (1): 1–10.

Sarver, A, and J DeRisi. 2005. "Fzf1p Regulates an Inducible Response to Nitrosative Stress in *Saccharomyces cerevisiae*[D] ". *Molecular Biology of the Cell* 16 (10): 4781–91.

Sengupta, R, and A Holmgren. 2012. "The Role of Thioredoxin in the Regulation of Cellular Processes by *S*-Nitrosylation." *Biochimica et Biophysica Acta - General Subjects* 1820 (6): 689–700.

Shiva, S. 2013. "Nitrite: A Physiological Store of Nitric Oxide and Modulator of

Mitochondrial Function." *Redox Biology* 1 (1): 40–44.

Stamler, Jonathan S, Daniel I Simon, John A Osborne, Mark A Mullins, O Jaraki, T Michel, David J Singel, and J Loscalzo. 1992. "*S*-Nitrosylation of Proteins with Nitric Oxide: Synthesis and Characterization of Biologically Active Compounds". *Proceedings of the National Academy of Sciences of the United States of America* 89: 444-8.

Sun, J, L Xu, J P Eu, J S Stamler, and G Meissner. 2003. "Nitric Oxide, NOC-12, and *S*-Nitrosoglutathione Modulate the Skeletal Muscle Calcium Release Channel/Ryanodine Receptor by Different Mechanisms. An Allosteric Function for O_2 in *S*-Nitrosylation of The Channel. *The Journal of Biological Chemistry* 278 (10): 8184-9.

Thippeswamy, T, J S McKay, J P Quinn, and R Morris. 2006. "Nitric Oxide, a Biological Double-Faced Janus- Is This Good or Bad?" *Histology and Histopathology* 21 (4–6): 445–58.

Tillmann, A, Neil A R Gow, and Alistair J P Brown. 2011. "Nitric Oxide and Nitrosative Stress Tolerance in Yeast." *Biochemical Society Transactions* 39 (1): 219–23.

Yamanaka, N, O Oda, and S Nagao. 1996. "Nitric Oxide Released from Zwitterionic Polyamine/NO Adducts Inhibits Cu^{2+}-Induced Low Density Lipoprotein Oxidation." *Federation of European Biochemical Societies letters* 398: 53-56.

Yoshikawa, Y, R Nasuno, N Kawahara, A Nishimura, D Watanabe, and H Takagi. 2016. "Regulatory Mechanism of the Flavoprotein Tah18-Dependent Nitric Oxide Synthesis and Cell Death in Yeast." *Nitric Oxide* 57: 85–91.

Yurgel, Svetlana N, N Sa, J Rice, and S Roje. 2014. "Assay for GTP Cyclohydrolase II Activity in Bacterial Extracts" *Bio-protocol* 4 (15): 1–8.

Yuste, J Enrique, E Tarragon, Carmen M Campuzano, and Francisco Ros-bernal. 2015. "Implications of Glial Nitric Oxide in Neurodegenerative Diseases" *Frontiers in Cellular Neuroscience* 9 (8): 1–13.

Zaffagnini, M, et al. 2013. "Mechanisms of Nitrosylation and Denitrosylation of Cytoplasmic Glyceraldehyde-3-Phosphate Dehydrogenase from *Arabidopsis Thaliana*." *Journal of Biological Chemistry* 288 (31): 22777–89.

Zhang, Y, L R Davies, S M Martin, W J Coddington, F J Jr Miller, G R Buettner, and R E Kerber. 2003. "The Nitric Oxide Donor *S*-Nitroso-N-Acetyl Penicillamine (SNAP) Increases Free Radical Generation and Degrades Left Ventricular Function After Myocardial Ischemia-Reperfusion. *Resuscitation* 59 (3): 345-52.

Zhou, S, T Narukami, M Nameki, T Ozawa, Y Kamimura, T Hoshino, and N Takaya. 2012. "Heme-Biosynthetic Porphobilinogen Deaminase Protects Aspergillus Nidulans from Nitrosative Stress." *Applied and Environmental Microbiology* 78 (1): 103–9.

Zhou, S, T Narukami, S Masuo, M Shimizu, T Fujita, Y Doi, Y Kamimura, and N Takaya. 2013. "NO-Inducible Nitrosothionein Mediates NO Removal in Tandem with Thioredoxin." *Nature Chemical Biology* 9 (10): 657–65.